

The influence of human activities on streamflow reductions during the megadrought in Central Chile

Nicolás Álamos^{1,2,3}, Camila Alvarez-Garretón¹, Ariel Muñoz^{1,3,4}, Álvaro González-Reyes^{2,5,6,7}

¹Center for Climate and Resilience Research (CR2, FONDAP 1522A0001), Santiago, Chile

²Instituto de Ciencias de la Tierra ICT, Facultad de Ciencias, Universidad Austral de Chile

³Centro de Acción Climática, Pontificia Universidad Católica de Valparaíso

⁴Laboratorio de Dendrocronología y Estudios Ambientales, Instituto de Geografía, Pontificia Universidad Católica de Valparaíso, Chile

⁵Centro de Humedales río Cruces CEHUM, Universidad Austral de Chile, Chile

⁶Laboratorio de Dendrocronología y Cambio Global, Universidad Austral de Chile, Valdivia, Chile

⁷Centro de Investigación: Dinámica de Ecosistemas Marinos de Altas Latitudes - IDEAL, Chile

Correspondence to: Camila Alvarez Garretón (calvarezgarreton@gmail.com)

Abstract. ~~Central~~Since 2010, central Chile has experienced a protracted megadrought ~~since 2010 (up to date)~~, with annual precipitation deficits ranging from 25% to 70%. ~~Drought~~An intensification of drought propagation has been ~~intensified during this time, with streamflow reductions up to 30% larger than those expected from historical records. This intensification has been attributed to the effect of cumulative effect of precipitation deficits associated linked to catchment memory in near-natural basins of central Chile. However, Yet, the additional effect influence of water extractions on drought intensification in disturbed basins remains an open challenge. In this is still unclear. Our study, we assess the effects of assesses climate and water use effects on streamflow reductions during the last three decades in a high human influence period (1988-2020) in four major agricultural basins in central Chile, with particular focus on the ongoing megadrought. We address this. We performed this attribution by contrasting observed streamflow observations (driven by climatic and water use) with near-natural streamflow simulations (driven mainly by climate) representing the discharge that what would have occurred without water extractions. Near-natural streamflow estimations are were obtained from rainfall-runoff models trained over a reference period with low human intervention (1960-1988). We characterise Annual and seasonal streamflow reductions were examined before and after the megadrought onset, and hydrological droughts driven by precipitation and human activities during the drought events were characterized for the complete evaluation period (1988-2020) in terms of the their frequency, duration and intensity of near-natural and observed seasonal streamflow deficits, respectively.~~

Definición de estilo: Normal

Definición de estilo: Texto de globo: Espacio Después 0 pto

Definición de estilo: Revisión

Con formato: Derecha: -0,11"

Con formato: Inglés (Reino Unido)

Con formato: Inglés (Reino Unido)

Con formato: Izquierda

Con formato: Color de fuente: Automático

Con formato: Borde: Superior: (Sin borde), Inferior: (Sin borde), Izquierda: (Sin borde), Derecha: (Sin borde), Entre : (Sin borde), Punto de tabulación: No en 3,13" 6,27"

28 Our results show that before the megadrought onset (1988-2009), ~~the mean annual deficits in observed~~ streamflow ~~in the four~~
29 ~~basins was ranged between~~ 2 to 20% ~~lower than~~ across the ~~streamflow during the undisturbed period. Between~~ study basins, and
30 ~~that~~ 81 to 100% of ~~these larger~~ those deficits were explained by water extractions. During the megadrought (2010-2020),
31 ~~streamflow was reduced~~ the mean annual deficits in a range of ~~observed streamflow were~~ 47 to 76 % among the ~~different~~ basins,
32 ~~compared to the reference period.~~ During this time, the ~~climatic contribution to streamflow reductions increased and water~~
33 ~~extractions had a lower~~ relative contribution ~~of precipitation deficits on streamflow reduction increased while the contribution of~~
34 ~~water extractions decreased~~, accounting for 27 to 51% of ~~streamflow reduction. During the~~ streamflow reduction. Regarding
35 ~~drought events during the~~ complete evaluation period, ~~we show~~ that human activities have amplified ~~the~~ drought
36 propagation ~~of droughts~~, with ~~more than~~ almost double the ~~frequency, duration, and~~ intensity of hydrological droughts in some
37 basins, compared to those expected by precipitation deficits only. We conclude that while the primary cause of streamflow
38 reductions during the megadrought has been the lack of precipitation, water uses have not diminished during this time, causing
39 an exacerbation of the hydrological drought conditions and aggravating their impacts on ~~human water consumption, economic~~
40 ~~activities, accessibility in rural communities~~ and natural ecosystems. ▲

Con formato: Fuente de párrafo predeter.

Con formato: Inglés (Reino Unido)

41 1 Introduction

42 The fluxes of the water cycle vary and change in time and space, as well as the anthropic activities affecting those fluxes, leading
43 to a co-evolving hydrosocial cycle (Linton and Budds, 2014; Budds, 2012) that defines the state of the hydrological system (Van
44 Loon et al., 2016). Observational evidence in different regions indicates that hydrological cycles are being affected by climate
45 change and human activities. Climate change has led to changes in precipitation patterns worldwide (Fleig et al., 2010; Kingston
46 et al., 2015), while human activities have altered the spatiotemporal distribution of water resources (Van Loon et al., 2022). This
47 can lead to water scarcity problems, particularly when precipitation deficits occur in regions that concentrate water consumption
48 requirements.

49 ~~The alterations in the water cycle may also affect the occurrence of droughts, which are defined as a deficit of water relative to~~
50 ~~normal conditions and can be identified in different components of the hydrological cycle.~~ While meteorological droughts
51 (precipitation deficits) are mainly controlled by regional climate, hydrological droughts (streamflow, and groundwater deficits)
52 are also influenced by catchment characteristics and water uses. In this way, under similar meteorological conditions, the severity
53 of hydrological droughts and their impacts on society can vary significantly within the territory (Van Lanen et al., 2013).

Con formato: Izquierda

Con formato: Color de fuente: Automático

Con formato: Borde: Superior: (Sin borde), Inferior: (Sin borde), Izquierda: (Sin borde), Derecha: (Sin borde), Entre : (Sin borde), Punto de tabulación: No en 3,13" 6,27"

54

55 Most drought analyses consider climate variability as a main driver of drought, however, increasing focus has been given to
56 assessing the compounding effects of climate variability and human activities on water resources and drought propagation (Van
57 Loon et al., 2016; Wanders and Wada, 2015; Zhao et al., 2014). Anthropogenic activities, such as irrigation, urbanization, land use
58 changes, and water infrastructure (e.g., reservoirs or water transfer channels) affect runoff mechanisms (Huang et al., 2016) and
59 can lead to a higher frequency of hydrological droughts (Alvarez-Garreton et al., 2021; Ward et al., 2020). ~~A notable example~~
60 An example of this is the Yellow river basin in China, where despite no significant rainfall deficits have occurred in recent years,
61 a hydrological drought with historical minimum streamflow levels is being observed, which has been mainly driven by anthropic
62 activities in the basin (Huang et al., 2016; Kong et al., 2016; Li et al., 2019; Liu et al., 2016; Zhao et al., 2014).

63 Advancing our understanding of hydrological droughts as a complex process depending on the interaction between climatic,
64 biophysical, and anthropic drivers is critical to ~~assess a catchment's~~ assessing catchment's vulnerability to droughts,
65 ~~mitigate~~ mitigating their occurrence, and ~~design~~ designing adaptation plans. While all these drivers influence the propagation and
66 impacts of droughts, ~~adaptation and mitigation~~ water management plans mainly influence ~~on~~ human activities and their local
67 disturbances to the hydrological cycle. Therefore, it is critical to address the scientific challenge of understanding the influence
68 of human activities on the hydrological cycle and quantifying their impacts.

69 To address this challenge, in this paper we focus ~~in~~ on central Chile (29°-35°S; Fig. 1), a region where the signal of anthropic
70 climate change is leading to an increase in mean temperature, increasing of heatwaves events, and a sustained decrease in
71 precipitation (Boisier et al., 2018; Bozkurt et al., 2017; Garreaud et al., 2017, 2020; González-Reyes et al., 2023). The drying
72 trend has led to the so-called megadrought, affecting the country since 2010, with annual precipitation deficits ranging between
73 25% and 70% (Garreaud et al., 2020, 2017). This meteorological drought in central Chile has propagated across the terrestrial
74 system, leading to hydrological droughts and water scarcity problems that vary across the territory (Alvarez-Garreton et al.,
75 2021; Duran-Llacer et al., 2020; Muñoz et al., 2020; Barría et al., 2021b).

76 ~~For example, in~~ In the Petorca river basin, located in the Valparaiso region in central Chile, Muñoz et al. (2020) found that during
77 the megadrought, streamflow, and water bodies ~~off~~ from the upper parts of the basin were less affected than the mid and low areas
78 of the valley, where most of the agriculture is located. However, the authors did not make a formal attribution study to
79 disentangle about the role of water consumption and climate on streamflow reduction. Another study was conducted on the

Con formato: Derecha: -0,11"

Con formato: Inglés (Reino Unido)

Con formato: Izquierda

Con formato: Color de fuente: Automático

Con formato: Borde: Superior: (Sin borde), Inferior: (Sin borde), Izquierda: (Sin borde), Derecha: (Sin borde), Entre : (Sin borde), Punto de tabulación: No en 3,13" 6,27"

80 Aculeo Lake, a natural reservoir in central Chile that dried up during the ongoing megadrought. ~~Barría et al. (2021b)~~ Barría et al
81 (2021b) performed an attribution exercise ~~and used~~ by using the Water Evaluation and Planning System (WEAP) hydrological
82 model and concluded that climate was the primary factor explaining the lake's drying, while water demand has remained stable
83 over the past few decades. ~~Another study reported that basins with larger human intervention within this region exhibited lower~~
84 ~~runoff sensitivities to precipitation compared to less disturbed ones (Alvarez-Garreton et al., 2018). In that study, the authors~~
85 ~~attributed this phenomenon to the alteration of runoff generation mechanisms associated with water withdrawals and reservoirs.~~
86 Furthermore, higher than expected streamflow reductions during the megadrought have also been observed in near-natural
87 basins. Alvarez-Garreton et al. (2021) reported the effects of catchment memory in snow-dominated catchments in Central Chile,
88 where the accumulation of the persistent precipitation deficits led to less streamflow than expected from observations during
89 previous single-year meteorological droughts. ~~Although there~~ These studies have ~~been some insights of~~ advanced our
90 ~~understanding about~~ the role of catchments and anthropic characteristics in the megadrought's propagation, ~~the impact~~ however,
91 ~~further studies are still required to robustly assess the impacts~~ of human activities on streamflow reduction and drought conditions
92 in the major basins of central Chile ~~remains unclear~~.

93 In this article, we quantify the relative effects of climate and water extractions on streamflow reduction ~~during the megadrought~~
94 ~~(2010-2020) and before it (1988-2010)~~ in four major agricultural basins in central Chile. ~~We analyse a period with high human~~
95 ~~influence within the study basins (1988-2020), and assess how the relative effects of climate and water extractions change before~~
96 ~~and after the megadrought onset~~. Additionally, we assess the influence of water extractions on the intensity, frequency, and
97 duration of hydrological droughts for the ~~same~~ complete evaluation period. To achieve this, we follow the approach proposed by
98 Van Loon et al. (2022) and compare streamflow observations with a near-natural simulated ~~flow~~ streamflow representing the
99 discharge that would have occurred without human influences. ~~Hydrological droughts are identified by streamflow deficit using~~
100 ~~a threshold determined from the near-natural scenario, allowing for better identification of human impacts (Van Loon, 2016).~~

101 2 Methods and data

102 2.1 Study area

103 The study was conducted in four major basins located between 29° and 33°S (Fig. 1): The Elqui, Limarí, and Choapa basins in
104 the Coquimbo region, and the Aconcagua basin in the Valparaíso region. These basins fall within semi-arid (Coquimbo region)

Con formato: Izquierda

Con formato: Color de fuente: Automático

Con formato: Borde: Superior: (Sin borde), Inferior: (Sin
borde), Izquierda: (Sin borde), Derecha: (Sin borde),
Entre : (Sin borde), Punto de tabulación: No en 3,13"
6,27"

105 and Mediterranean (Valparaiso region) climate zones, which are particularly vulnerable to droughts due to the majority of annual
106 precipitation occurring during the winter season concentrated on a few storm events (Garreaud et al., 2017).

107 All catchments feature a snow-rain-fed hydrologic regime. The Aconcagua basin also has a large glacier area (192 km²) that
108 contributes to streamflow, especially during dry summers (Crespo et al., 2020). The study basins have experienced precipitation
109 deficits of 25-70% and streamflow deficits of up to 70% during the megadrought that has affected the region since 2010 (Alvarez-
110 Garreton et al., 2021; Garreaud et al., 2020, 2017).

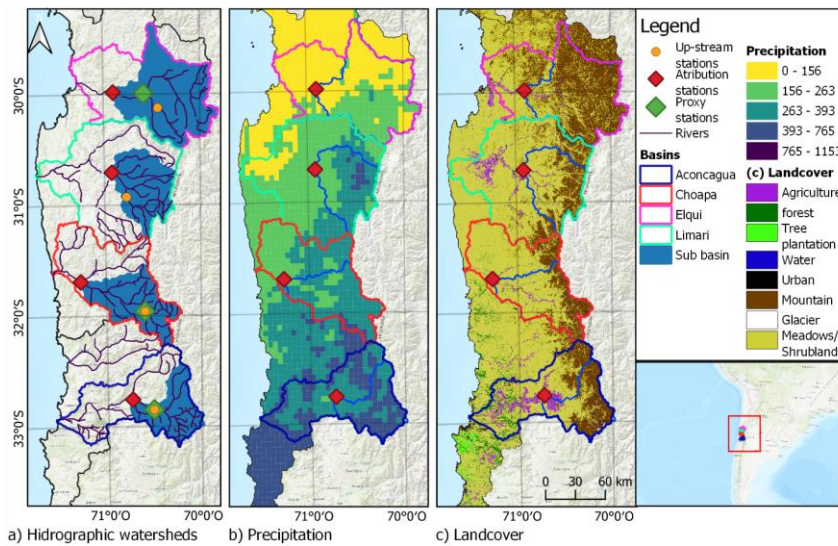
111 According to the data provided by the water security platform from the Center for Climate and Resilience Research
112 (www.seguridadhidrica.cl), agriculture is the primary productive sector and the main consumer of water resources within these
113 basins. Agricultural landsland cover areas of 152 km², (total catchment area of 9800 km²), 605 km², (total catchment area of
114 11800 km²), 313 km², (total catchment area of 8124 km²), and 582 km², (total catchment area of 7200 km²), and their annual
115 water consumption at present corresponds to 3.25 m³/s, 14.3 m³/s, 6.48 m³/s, and 15.72 m³/s, in the Elqui, Limarí, Choapa, and
116 Aconcagua basins, respectively. Avocado and table vine species are the main consumers in the Aconcagua basin, while the
117 Limarí basin has a higher demand from permanent forage species, table vine, and citrus plantations.

Con formato: Derecha: -0,11"

Con formato: Izquierda

Con formato: Color de fuente: Automático

Con formato: Borde: Superior: (Sin borde), Inferior: (Sin borde), Izquierda: (Sin borde), Derecha: (Sin borde), Entre : (Sin borde), Punto de tabulación: No en 3,13" 6,27"



118

119 **Figure 1.** Panel a) shows the four main basins of the study area and the streamflow gauges used for the analyses. The red diamonds
 120 indicate the stations used to characterise each basin; the green diamonds are the gauges used as predictors for filling in monthly
 121 streamflow data (note that in the Limari catchment, no gap-filling process was made, leading to the absence of a predictor gauge
 122 station; Sect. 2.2); and the orange circles are the up-stream stations used in the rainfall-runoff ratio analysis (Sect. 2.3). The basin area
 123 covered by the red diamond gauge is painted blue. Panel b) presents the mean annual precipitation (mm/yr) from the CR2MET dataset
 124 for the period 1980-2010. Panel c) shows the gridded land cover dataset from Zhao et al. (2016). Base map source: Esri, 2017.

125

2.2 Data

126

Times-series of monthly streamflow and runoff (streamflow normalised by catchment area) were obtained from the CAMELS-
 CL dataset. Catchment boundaries and times series of total monthly streamflow normalized by catchment area (in mm/month)
 were obtained from the CAMELS-CL dataset (Alvarez-Garreton et al., 2018; available at: <https://camels.cr2.cl/>) for the period
 April 1960 – March 2020. Total monthly precipitation for the same period was obtained from the CR2MET dataset version 2.5
 at a 5 x 5 km grid resolution (Boisier, 2023) and averaged across the basin boundaries. Catchment-scale monthly

130

Con formato: Subrayado

Con formato: Derecha: -0,11"

Con formato: Izquierda

Con formato: Color de fuente: Automático

Con formato: Borde: Superior: (Sin borde), Inferior: (Sin borde), Izquierda: (Sin borde), Derecha: (Sin borde), Entre : (Sin borde), Punto de tabulación: No en 3,13" 6,27"

131 evapotranspiration (ET) was computed based on the ECMWF surface re-analysis ERA5-Land dataset, available at a horizontal
132 resolution of 10 km (Muñoz-Sabater et al., 2021) from April 1960 to March 2020. For each study basin, we selected the most
133 downstream streamflow gauge station having more than 80% of streamflow records for the 1960-2020 period (see Fig. 1). Gaps
134 in monthly streamflow of downstream gauges (red diamonds in Fig. 1a) were filled based on linear regression models, using the
135 basin's precipitation and the streamflow of an upstream gauge with a strong correlation with the considered station (green
136 diamonds in Fig. 1a) as predictors. The linear regressions resulted in coefficients of determination larger than 0.8 in Elqui,
137 Choapa, and Aconcagua basins.

138 Streamflow and basin-averaged precipitation and ET were computed for hydrological years (April to March in Chile) and for
139 wet and dry seasons. The wet season is defined from April to August, while the dry season corresponds to the months between
140 September and March. Annual (seasonal) streamflow values were computed when the 12 (6) months had valid data.

141 To account for human intervention within the basins, we analysed annual water uses from industry, energy, mining, livestock,
142 drinking water sectors, as well as water evaporation from lakes and reservoirs for the period 1960-2020 obtained from the water
143 security platform from the Center for Climate and Resilience Research (www.seguridadhidrica.cl). All variables with a different
144 spatial resolution than the basin (whether gridded or administrative units) were calculated for the basin considering the weighted
145 average of the variable within the basin surface.

146 **2.3 Near-natural streamflow modelling and attribution exercise**

147 The attribution exercise to quantify the climatic and human contributions on streamflow reductions is schematized in Fig. 2.
148 Near-natural streamflow simulations were obtained by rainfall-runoff statistical models trained in a period when anthropic
149 activities had low water consumption (Sharifi et al., 2021; Zhao et al., 2014).

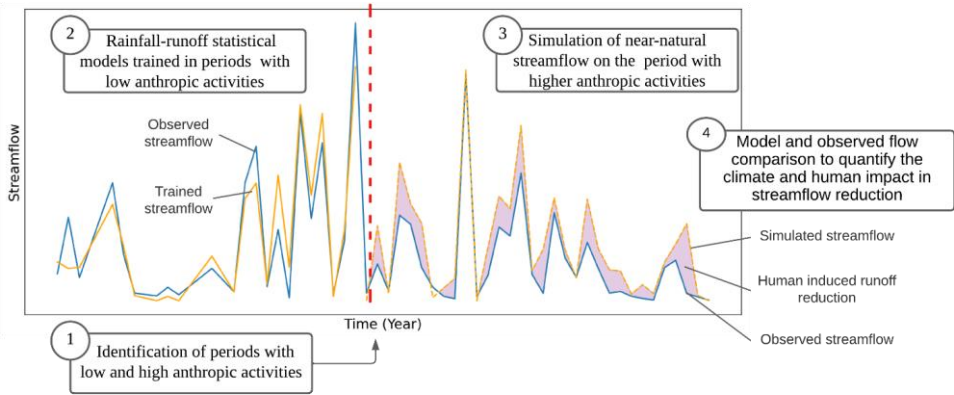
Con formato: Derecha: -0,11"

Con formato: Izquierda

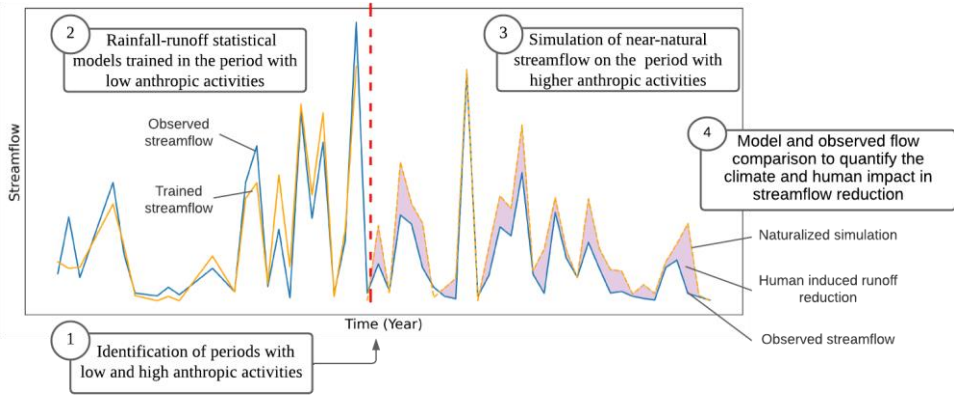
Con formato: Color de fuente: Automático

Con formato: Borde: Superior: (Sin borde), Inferior: (Sin
borde), Izquierda: (Sin borde), Derecha: (Sin borde),
Entre : (Sin borde), Punto de tabulación: No en 3,13"
6,27"

150



151



152

153

Figure 2. Flowchart of the steps to quantify the human contribution to streamflow reduction based on comparing a near-natural simulated streamflow with the observed streamflow on a period of high anthropic activities.

Con formato: Derecha: -0,11"

Con formato: Izquierda

Con formato: Color de fuente: Automático

Con formato: Borde: Superior: (Sin borde), Inferior: (Sin borde), Izquierda: (Sin borde), Derecha: (Sin borde), Entre : (Sin borde), Punto de tabulación: No en 3,13" 6,27"

2.3.1 Selection of low-influence ~~training~~reference periods

For each basin, we identified low human intervention periods based on the regime shifts of streamflow, precipitation, and anthropic variables (Sect. 2.2). ~~The non-parametric Buishand break point test (Buishand, 1982) was applied to identify regime shifts.~~ water uses (Sect. 2.2). ~~The non-parametric Buishand break point test (Buishand, 1982) was applied to identify these shifts.~~ Buishand is a statistical homogeneity test method that checks if two (or more) datasets come from the same distribution. In this way, the test can detect breakpoints where the distribution of a dataset changes. We applied the Buishand test to each time series during the 1960-2020 periods. To identify multiple breakpoints, we iterated the test in the sub-periods before and after the previous breakpoint until no breakpoints with a significance level at p-value < 0.05. For the Buishand test, we used the pyHomogeneity Python library (~~Shourov, 2020~~)(Shourov, 2020).

~~Subsequently, a singular training period was selected~~In order to select periods with minimal human activities, it is important to identify breakpoints in the streamflow time series that are not primarily explained by climate shifts. To account for this, we selected a unique training period across basins based on the identification of concurrent breaking points in both streamflow and human activities time series, while ensuring the absence of discernible precipitation shifts. By employing this approach, we ensure the selection of streamflow breakpoints that are not predominantly influenced by climatic variations.

To ensure that the chosen period of analysis is not dependent on the specific statistical test employed, we conducted a sensitivity analysis using the Sequential T-test Analysis of Regime Shifts (STARS) at a monthly time scale for both precipitation and streamflow time series (~~Rodionov, 2004~~). ~~The STARS V6.3 Excel macro application, available at <https://sites.google.com/view/regime-shift-test> was utilized to perform the Rodionov~~(Rodionov, 2004). ~~The STARS V6.3 Excel macro application, available at <https://sites.google.com/view/regime-shift-test> was utilized to perform the STARS~~ test.

2.3.2 Climate and human contribution to streamflow reduction

Assuming that the effects of climate and local human activities on streamflow generation are independent, the observed streamflow (Q_{obs}) can be disaggregated as follows (Kong et al., 2016):

$$Q_{obs} = Q_{nn} + \Delta Q_{human} \quad (1)$$

Con formato: Derecha: -0,11"

Con formato: Izquierda

Con formato: Color de fuente: Automático

Con formato: Borde: Superior: (Sin borde), Inferior: (Sin borde), Izquierda: (Sin borde), Derecha: (Sin borde), Entre : (Sin borde), Punto de tabulación: No en 3,13" 6,27"

177 Where Q_{nn} corresponds to a climatic-induced streamflow, referred as near-natural streamflow in this paper, and ΔQ_{human} is the
 178 human-induced effect on streamflow. In this study, near-natural streamflow in Eq.1 is estimated from linear rainfall-runoff
 179 regressions trained ~~in~~during the low-influence reference period defined in Sect. 2.3.1. To account for pluvial and snowmelt
 180 runoff generation processes, we implemented seasonal rainfall-runoff models: ~~considering the total streamflow and rainfall in~~
 181 ~~the six-month periods defined in Sect 2.2 as dependent and independent variables, respectively.~~ In several snow-dominated
 182 basins in central Chile, the winter flows continue to be fed by the snow ~~accumulation of~~melt from the previous hydrological
 183 year, especially when the previous year was wetter than normal (Alvarez-Garreton et al., 2021). Given this, ~~to model~~winter
 184 ~~flows, flow models include~~ winter precipitation ~~off~~from the previous year ~~is added as a predictor.~~ The models representing near-
 185 natural summer (\hat{Q}_{summer}) and near-natural winter streamflow (\hat{Q}_{winter}) were defined for year t as follows:

$$\hat{Q}_{summer} \hat{Q}_{summer}(t) = a_0 + a_1 P_{winter}(t) \quad (2)$$

$$\hat{Q}_{winter} \hat{Q}_{winter}(t) = b_0 + b_1 P_{winter}(t) + b_2 P_{winter}(t - 1) \quad (3)$$

188 The coefficients in Eq. 2 and 3 were obtained by least square errors method during the training period. Based on this, the human
 189 influence during ~~an~~the evaluation (high-influence) period ~~is~~was obtained as:

$$\Delta Q_{human} = Q_{obs} - \hat{Q}_{nn} \hat{Q}_{nn} \pm \varepsilon \quad (4)$$

191 where \hat{Q}_{nn} is the simulated near-natural streamflow (~~seasonal concatenation of~~ Eq. 2 and 3) and $-\varepsilon$ represents the uncertainty
 192 ~~off~~from the regression model ~~parameters~~. The attribution exercises were performed by applying Eq. 4 during the evaluation
 193 period. ~~In the results of the attribution exercise (Sect 3.3; Fig 7), hydroclimatic variables are depicted as anomalies computed as~~
 194 ~~the percentage difference from their mean values during the reference period (1960-1988).~~ Noteworthy that multiple regression
 195 equations with different functional forms ~~and variables~~—(including ~~a Box-Cox transformation to the seasonal and annual~~
 196 ~~streamflow to account for potential non linearities between precipitation and streamflow) and variables (such as~~
 197 ~~evapotranspiration and temperature-)~~ were tested for representing near-natural streamflow during the reference period. ~~(see~~
 198 ~~Appendix A).~~ The linear rainfall-runoff regressions from equations (2) and (3) were those with a higher r^2 , and all variables ~~were~~
 199 statistically significant at a p-value of 0.05.

Con formato: Fuente: Times New Roman

Con formato: Fuente: Times New Roman

Con formato: Fuente: Times New Roman

Con formato: Izquierda

Con formato: Color de fuente: Automático

Con formato: Borde: Superior: (Sin borde), Inferior: (Sin borde), Izquierda: (Sin borde), Derecha: (Sin borde), Entre : (Sin borde), Punto de tabulación: No en 3,13" 6,27"

200 It should be noted that the near-natural streamflow estimations from Eq. 2 and 3 assume a stationary rainfall-runoff relationship.
201 However, recent evidence in this region has shown that, under protracted drought conditions, ~~there is a~~ non-stationary catchment
202 response modulated by catchment memory ~~that can emerge, resulting in~~ larger streamflow reductions ~~than~~ those
203 expected from single-year precipitation deficits ~~before the megadrought~~ (Alvarez-Garreton et al., 2021). This evidence
204 corresponds to the headwater near-natural basins located upstream of the human influenced basins selected in this study. To
205 assess whether our analyses over the complete basins are potentially biased by non-stationary catchment responses, we
206 ~~compare~~compared the rainfall-runoff ratios (mean annual ~~runoff~~observed streamflow normalised by mean annual precipitation)
207 during the evaluation period before (1988-2010) and after the megadrought onset (2010-2020), in both the upper and lower
208 sections of each basin. These sections were defined by the streamflow gauges highlighted in orange circles and red diamonds
209 in Fig. 1, respectively.

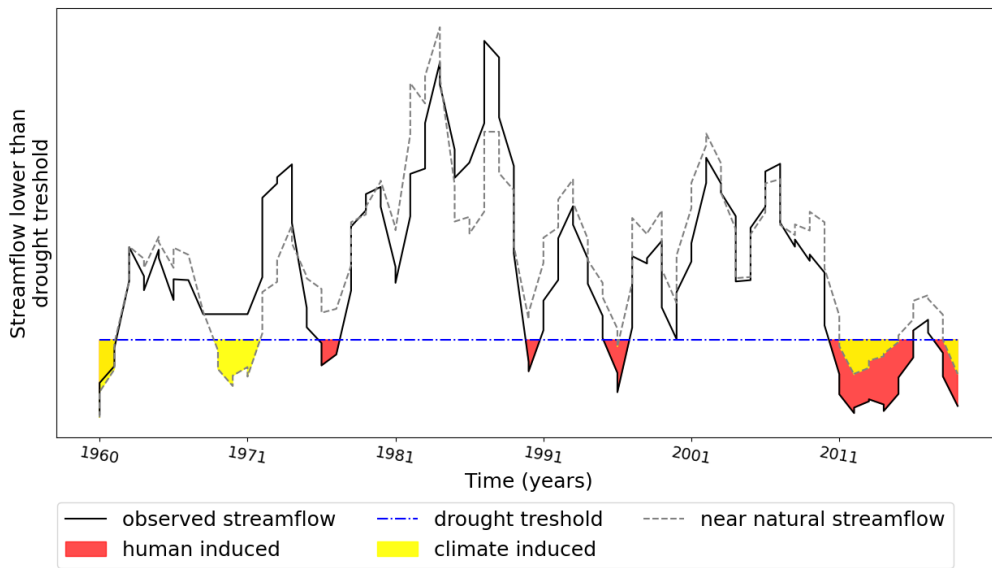
210 **2.4 Hydrological drought events characterisation**

211 To quantify the impact of human activities on hydrological droughts, (schematised in Fig. 3), we compared the characteristics
212 of the observed and the near-natural streamflow deficits during drought events, including their frequency (number of drought
213 events), duration (average, maximum and total seasons), and intensity (i.e., deficit of volume) across the evaluation period. In
214 this way, we ~~can assess~~assessed the ~~relative~~ influence of ~~climate and~~ human activities ~~on the~~over observed streamflow
215 ~~deficits, hydrological droughts by calculating the relative difference in each drought characteristic (DC) in the observed and near~~
216 natural scenario as ~~sehematised in Fig. 3, indicated eq. 5~~

Con formato: Izquierda

Con formato: Color de fuente: Automático

Con formato: Borde: Superior: (Sin borde), Inferior: (Sin borde), Izquierda: (Sin borde), Derecha: (Sin borde), Entre : (Sin borde), Punto de tabulación: No en 3,13" 6,27"



$$DC_{human} = \frac{DC_{obs} - DC_{nn}}{DC_{obs}} * 100 \text{ (5)}$$

217

218

Con formato: Izquierda

Con formato: Color de fuente: Automático

Con formato: Borde: Superior: (Sin borde), Inferior: (Sin borde), Izquierda: (Sin borde), Derecha: (Sin borde), Entre : (Sin borde), Punto de tabulación: No en 3,13" 6,27"

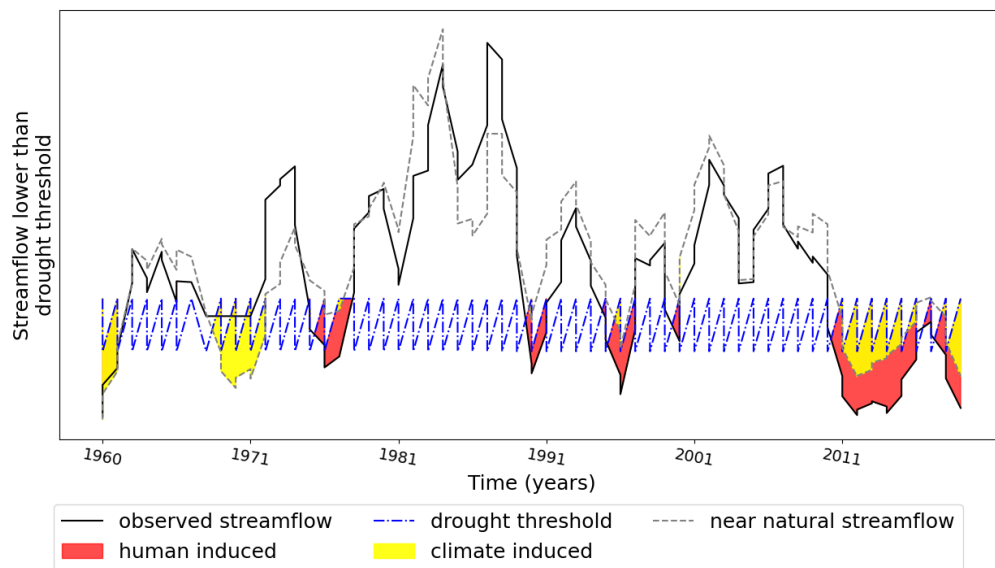


Figure 3. Example of drought periods with annual streamflow lower than a drought threshold. Three types of droughts are identified: climate-induced droughts, when near-natural streamflow simulations are below the threshold; human-induced droughts, where only observations are below the threshold; and human and natural induced, where both observations and near-natural estimations are below the threshold (adapted from Van Loon et al., 2016).

To identify drought events, thresholds based on percentiles of the flow duration curve are commonly used. For daily or monthly time series, a recommended threshold falls between the 70th and 90th percentile (Rangecroft et al., 2019; Van Loon et al., 2016; Van Loon, 2015). In this study, the 80th percentile of the seasonal flow series is adopted to define hydrological droughts. The threshold can be fixed or variable; we used the variable threshold to incorporate seasonality into the threshold (Rangecroft et al., 2019; Van Loon et al., 2019).

To identify hydrological drought events, we adopted a threshold approach, which defines drought events when the streamflow is below a specific percentile of the flow duration curve. For daily or monthly time series, a recommended threshold falls between

Con formato: Derecha: -0,11"

Con formato: Izquierda

Con formato: Color de fuente: Automático

Con formato: Borde: Superior: (Sin borde), Inferior: (Sin borde), Izquierda: (Sin borde), Derecha: (Sin borde), Entre : (Sin borde), Punto de tabulación: No en 3,13" 6,27"

231 the 70th and 90th percentile (Rangecroft et al., 2019; Van Loon et al., 2016; Van Loon, 2015). In this study, we adopted the 70th
232 percentile of the seasonal streamflow series. This lowest threshold allows for the selection of more drought events, which makes
233 statistical analysis more robust. The threshold can be fixed or variable; we used the variable threshold to incorporate seasonality
234 into the drought selection (Rangecroft et al., 2019; Van Loon et al., 2019).

235 To allow for a strict assessment of human influence on hydrological drought, the selected threshold should not account for human
236 activities (Rangecroft et al., 2019). If streamflow observations for the complete period were considered, human activities would
237 be included. On the other hand, if only the training low-influence periods were used to calculate the threshold, the climate
238 variability and drying trend of the complete period would not be represented by the threshold. Therefore, following the approach
239 of Rangecroft et al. (2019), we ~~defined~~ defined the drought threshold using the entire period of records (1960-2020) but considering
240 a ~~naturalised~~ naturalized regime. To this end, we used the ~~observed streamflow during the training period and the~~ near-natural
241 simulated streamflow during the ~~evaluation~~ whole period to establish the ~~80th~~ 70th percentile of the seasonal threshold.

242 3 Results

243 3.1 Low-influence ~~periods~~reference period

244 The series of annual streamflow, precipitation, total evapotranspiration (ET), and runoff coefficients (runoff normalised by
245 precipitation) are shown in Fig. 4. The Buishand test resulted in significant change points only in streamflow and ET. Three
246 change points were detected in all basins, the first between the years 1977-1978, the second one in 1988, and the last one between
247 years 1998-2010 years for the streamflow in all basins (Fig. 4), while a single change point was detected in 1973-1975 for ET
248 in all basins except Aconcagua- (Fig. 4d). The ~~Rodionov~~ Rodionov STARS test detected similar three change points in streamflow in 1977
249 -1981, 1988, and 2010, with the 1988 breakpoint presenting the higher R-shift index value.

250 ~~In order to select periods with minimal human activities, it is important to identify breakpoints in the streamflow time series~~
251 ~~that are not primarily explained by climate shifts. The streamflow breakpoint of 1977-1978 is disregarded since it is mainly~~
252 ~~due to climate. The streamflow breakpoint of 1977-1978 was disregarded since it is mainly due to climatic~~ drivers, as indicated
253 by the single ET breakpoint during that period. We can relate this to the great Pacific shift and the warm cycle of the Pacific
254 Decadal Oscillation (PDO) between 1977 and the mid-1990s (Kayano et al., 2009; Jacques-Coper and Garreaud, 2015;
255 González-Reyes et al., 2017). Additionally, the 2010 Aconcagua streamflow breakpoint is likely driven by the onset of the

Con formato: Derecha: -0,11"

Con formato: Izquierda

Con formato: Color de fuente: Automático

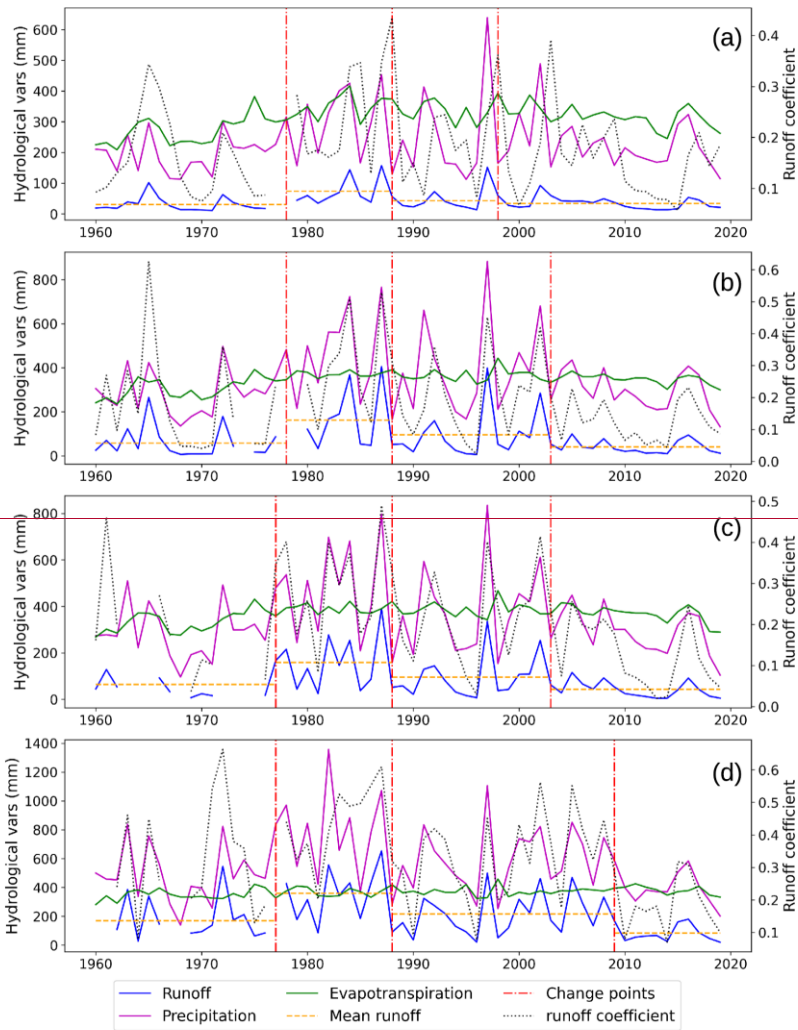
Con formato: Borde: Superior: (Sin borde), Inferior: (Sin
borde), Izquierda: (Sin borde), Derecha: (Sin borde),
Entre : (Sin borde), Punto de tabulación: No en 3,13"
6,27"

256 megadrought, which also affected the 2004 change points in the Limarí and Choapa Basins where lower precipitation was
257 observed even before the megadrought.

Con formato: Izquierda

Con formato: Color de fuente: Automático

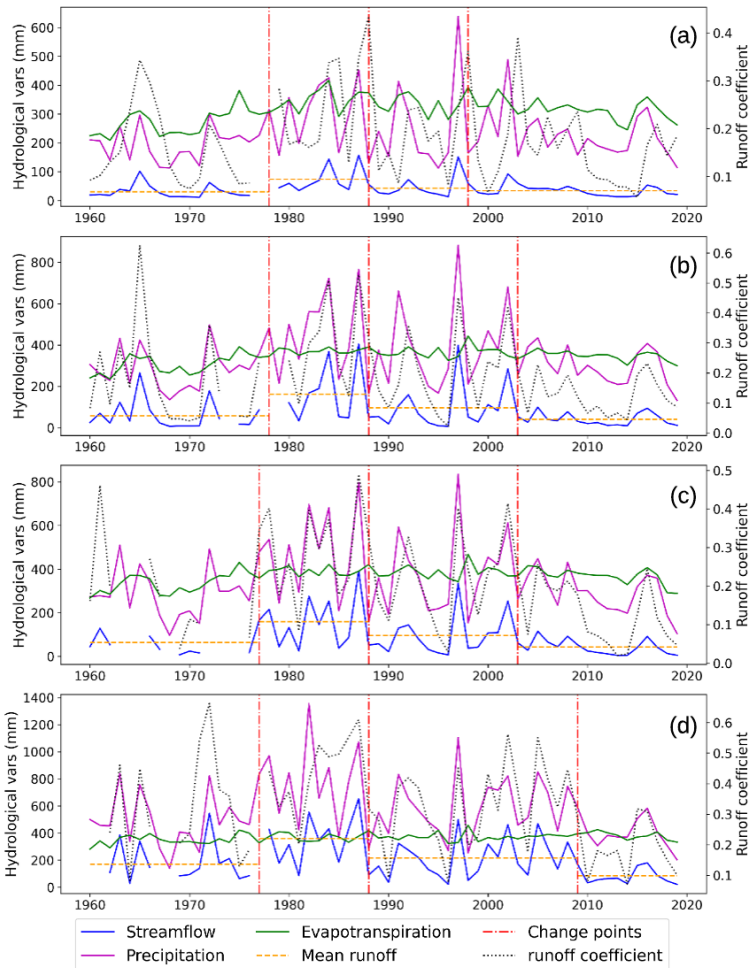
Con formato: Borde: Superior: (Sin borde), Inferior: (Sin borde), Izquierda: (Sin borde), Derecha: (Sin borde), Entre : (Sin borde), Punto de tabulación: No en 3,13" 6,27"



Con formato: Izquierda

Con formato: Color de fuente: Automático

Con formato: Borde: Superior: (Sin borde), Inferior: (Sin borde), Izquierda: (Sin borde), Derecha: (Sin borde), Entre : (Sin borde), Punto de tabulación: No en 3,13" 6,27"



Con formato: Izquierda

Con formato: Color de fuente: Automático

Con formato: Borde: Superior: (Sin borde), Inferior: (Sin borde), Izquierda: (Sin borde), Derecha: (Sin borde), Entre : (Sin borde), Punto de tabulación: No en 3,13" 6,27"

Figure 4. Annual streamflow, precipitation, evapotranspiration, and runoff coefficient during the complete period (1960-2020) for Elqui (a), Limarí (b), Choapa (c), and Aconcagua (d) Basins, respectively. The vertical red line indicates the years where significant change points (P value < 0.05) on streamflow distribution are detected by the Buishand test.

Regarding water use, breakpoints were observed in Elqui and Limarí in 1988 and 1992, respectively, mainly associated to the growth of the agricultural sector (Fig. 55a and b). In the Aconcagua basin, a breakpoint occurred in 1985 due to intensified water use by the mining and agriculture sectors- (Fig. 5d). Meanwhile, in the Choapa basin, a significant increase in mining water consumption since 2000 explains the time series breakpoint observed in that year- (Fig. 5c). The 1998 Elqui Basin streamflow breakpoint may be attributed to the construction of a dam upstream from the gauge station considered in this study (Fig. 55a). Based on these results, we used the 1988 streamflow breakpoint ~~observed~~detected in all basins to define the low-influence period of 1960-1988. In consequence, the evaluation period was defined between 1988 and 2020, characterised by greater ~~anthropogenic~~anthropic intervention and by the megadrought in its second half.

By comparing the hydroclimatic conditions of the study basins during the low-influence and evaluation periods, we see that the mean annual precipitation declined between 0 to 18% during these periods (Table 1). In contrast, the mean annual streamflow decreased by a range of 14 to 35%. If we examine summer streamflow, when agricultural water consumption is more intense, a reduction of 24 to 46% is observed. While the Aconcagua basin features the largest decrease in precipitation, the Choapa basin has the largest decrease in streamflow.

Basin	Mean annual precipitation (mm)			Mean annual runoff <u>streamflow</u> (mm)			Mean summer runoff <u>streamflow</u> (mm)		
	Low-influence period	Evaluation period	Difference	Low-influence period	Evaluation period	Difference %	Low-influence period	Evaluation period	Difference %
Elqui	232.83	232.73	0.0%	45.53	39,17	-15.9%	28.66	21.71	-24.3%
Limarí	355.13	336.78	-5.2%	95.91	66,92	-30.2%	54.50	33.87	-37.9%
Choapa	371.16	327.76	-11.7%	106.41	66,77	-37.2%	68.09	36.70	-46.1%
Aconcagua	634.61	533.76	-16%	258.42	173,87	-32.7%	193.29	119.82	-38.0%

Con formato: Derecha: -0,11", Espacio Después: 0 p
Borde: Superior: (Sin borde), Inferior: (Sin borde),
Izquierda: (Sin borde), Derecha: (Sin borde), Entre : (S
borde)

Con formato: Derecha: -0,11"

Tabla con formato

Con formato: Derecha: -0,11"

Con formato: Derecha: -0,11"

Con formato: Derecha: -0,11"

Con formato: Derecha: -0,11"

Con formato: Derecha: -0,11"

Con formato: Izquierda

Con formato: Color de fuente: Automático

Con formato: Borde: Superior: (Sin borde), Inferior: (Sin
borde), Izquierda: (Sin borde), Derecha: (Sin borde),
Entre : (Sin borde), Punto de tabulación: No en 3,13"
6,27"

276
277
278

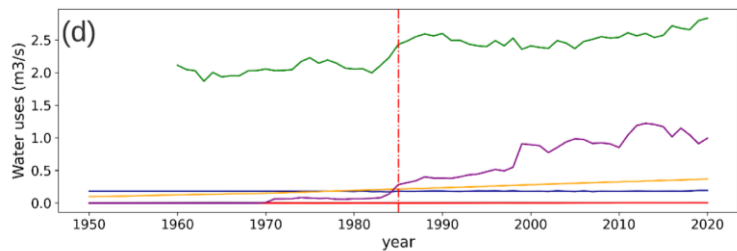
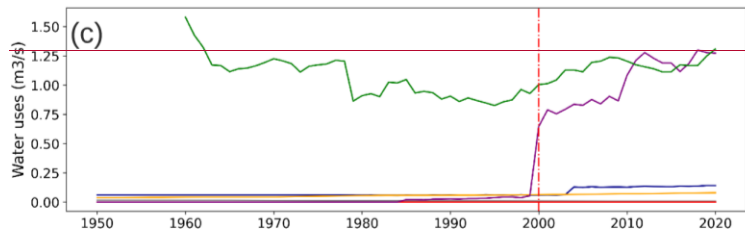
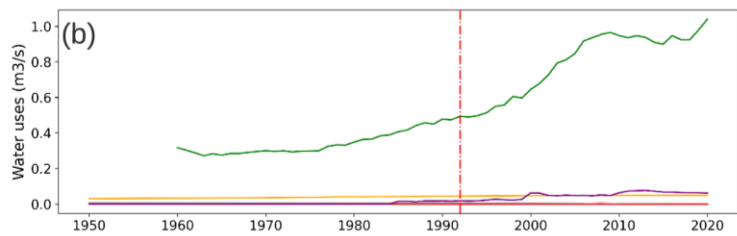
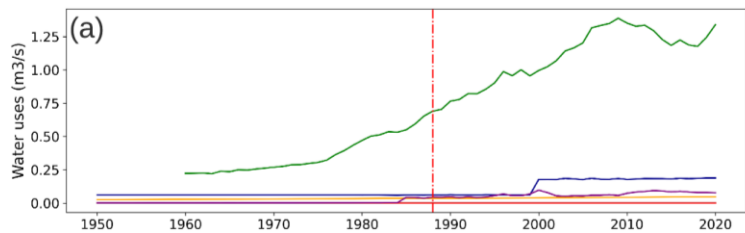
Table 1: Average annual precipitation, average annual streamflow, and average summer season streamflow for each basin in the low-influence reference period (1960-1988) and the evaluation period (1988-2020).

Con formato: Derecha: -0,11"

Con formato: Izquierda

Con formato: Color de fuente: Automático

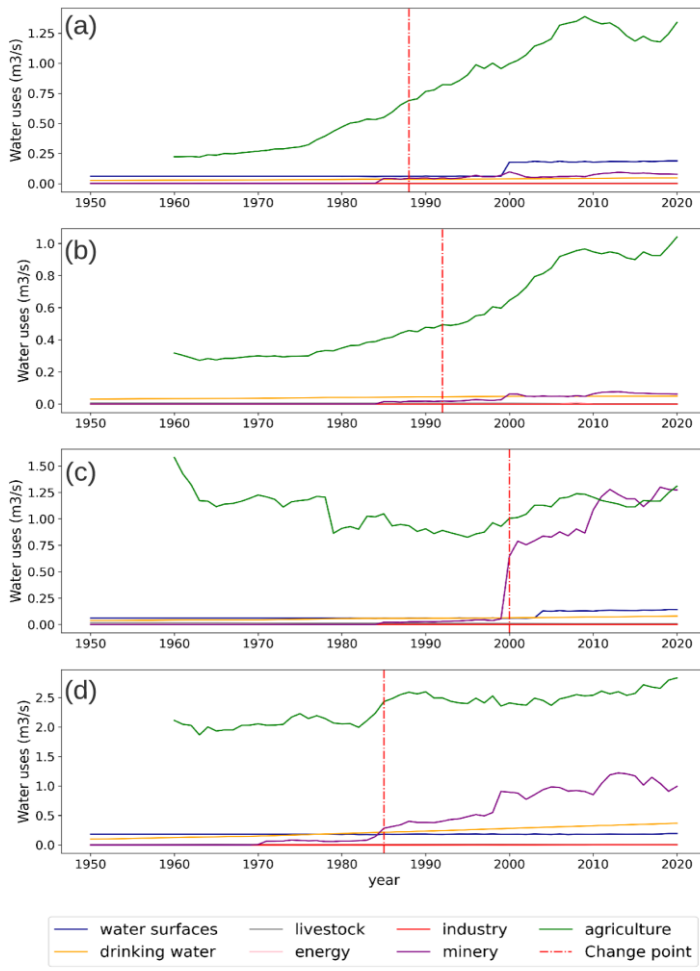
Con formato: Borde: Superior: (Sin borde), Inferior: (Sin borde), Izquierda: (Sin borde), Derecha: (Sin borde), Entre : (Sin borde), Punto de tabulación: No en 3,13" 6,27"



Con formato: Izquierda

Con formato: Color de fuente: Automático

Con formato: Borde: Superior: (Sin borde), Inferior: (Sin borde), Izquierda: (Sin borde), Derecha: (Sin borde), Entre : (Sin borde), Punto de tabulación: No en 3,13" 6,27"



Con formato: Izquierda

Con formato: Color de fuente: Automático

Con formato: Borde: Superior: (Sin borde), Inferior: (Sin borde), Izquierda: (Sin borde), Derecha: (Sin borde), Entre : (Sin borde), Punto de tabulación: No en 3,13" 6,27"

281 **Figure 5. Time series of water uses from different human activities in Elqui (a), Limarí (b), Choapa (c), and Aconcagua (d) basins,**
282 **respectively. These time series include water uses for industrial, agriculture, mining, energy, animals, water surfaces, and drinking**
283 **water sectors. The red line indicates a breakpoint in the total water use distribution.**

284 3.2 Near-natural streamflow estimation

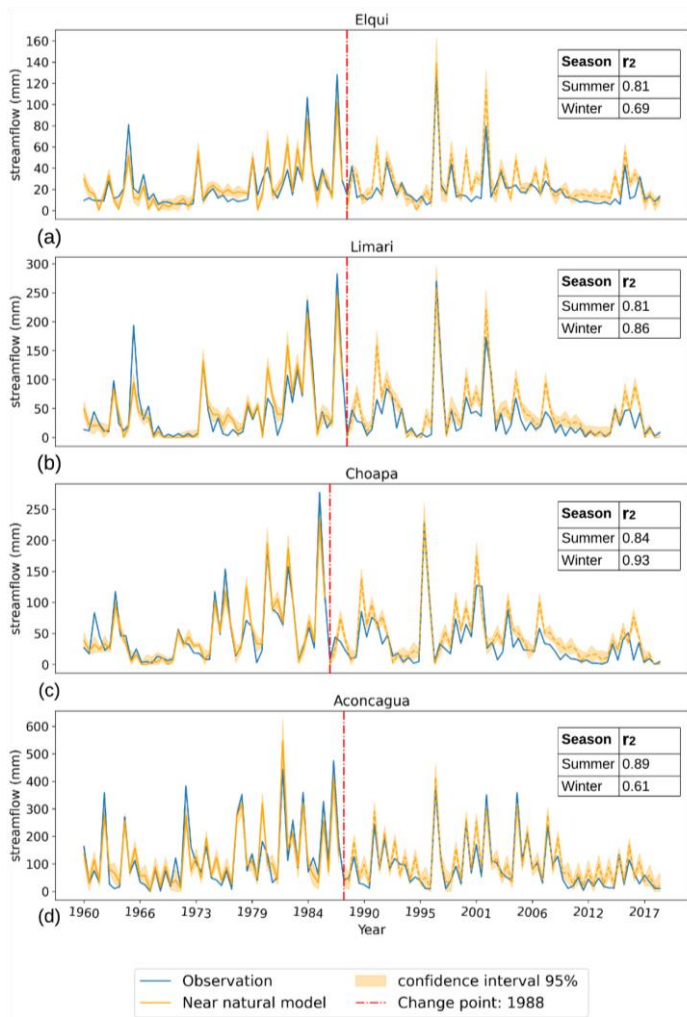
285 Near-natural simulated streamflow during the low-influence and evaluation periods for each basin is presented in Fig. 6. The
286 selected models (Sect. 2.3) were based on streamflow values without the Box-Cox transformation, since the transformed data
287 led to a reduction in model performance across all basins (Appendix A). The summer season estimations obtained from Eq. 2
288 had good performances during the training period, with mean biases of 0 to 5% and r^2 ranging from 0.8 to 0.89 for the different
289 basins. The winter season models resulted in lower performance, with mean biases of 0 to 0.63% and r^2 ranging from 0.61 and
290 0.93 among the study basins (Table 2).

Con formato: Derecha: -0,11"

Con formato: Izquierda

Con formato: Color de fuente: Automático

Con formato: Borde: Superior: (Sin borde), Inferior: (Sin borde), Izquierda: (Sin borde), Derecha: (Sin borde), Entre : (Sin borde), Punto de tabulación: No en 3,13" 6,27"



Con formato: Izquierda

Con formato: Color de fuente: Automático

Con formato: Borde: Superior: (Sin borde), Inferior: (Sin borde), Izquierda: (Sin borde), Derecha: (Sin borde), Entre : (Sin borde), Punto de tabulación: No en 3,13" 6,27"

Figure 6. Basin	Season	r ²	Mean bias
Elqui	Summer	0.81	-0.01%
	Winter	0.69	0%
Limarí	Summer	0.84	-5%
	Winter	0.86	0.63%
Choapa	Summer	0.89	-0.05%
	Winter	0.93	0.06%
Aconcagua	Summer	0.81	0%
	Winter	0.61	0%

Table 2: Seasonal model results in the calibration period.

The observed (continuous blue line) and near-natural simulated seasonal streamflow (continuous and dashed yellow line) for Elqui (a), Limarí (b), Choapa (c), and Aconcagua (d) basins, respectively. The continuous yellow line represents the simulated streamflow during the reference period, whose r² is presented on the legend. The dashed yellow line is the simulated streamflow during the evaluation period (defined by the change point in 1988). The yellow ban represents the 95% confidence interval of the simulated streamflow.

To test examine the potential biases induced by influence of non-stationary catchment response during the megadrought on the interpretation of our results, Table 32 shows the rainfall-runoff ratios during the evaluation period before (1988-2010) and after the megadrought onset (2010-2020), in the upper and lower sections of each basin, respectively. These results indicate that the mean rainfall-runoff ratios declined across all sections and the upper and lower sections (defined by up-stream and attribution stations from Fig. 1a, respectively) of all basins during the megadrought, however, the reduction in the upper sections, (with low human intervention), mostly attributed to endogenous runoff mechanisms and hydrological memory, is less significant than that those observed downstream. Specifically, the (intervened basin). The changes in downstream rainfall-runoff ratios are nearly four times greater than the upper stream changes in the Aconcagua and Elqui basins, more than twice as much in Choapa, and 1.6 times greater at in the Limarí station, which is the sub-basin with the lowest level of human activity in our attribution exercise. This indicates that while endogenous runoff mechanisms, such as hydrological memory, may contribute to larger streamflow deficits during prolonged drought in near-natural basins, human activities in the downstream basins are inducing a larger impact in runoff generation during the megadrought.

Basin	Elqui		Limarí		Choapa		Aconcagua	
Section	Upper	Lower	Upper	Lower	Upper	Lower	Upper	Lower

Con formato: Derecha: -0,11"

Tabla con formato

Con formato: Derecha: -0,11"

Con formato: Izquierda

Con formato: Color de fuente: Automático

Con formato: Borde: Superior: (Sin borde), Inferior: (Sin borde), Izquierda: (Sin borde), Derecha: (Sin borde), Entre : (Sin borde), Punto de tabulación: No en 3,13" 6,27"

Period	1988 -2010	0.42	0.19	0.41	0.18	0.58	0.21	0.75	0.33
	2010 -2020	0.38	0.12	0.31	0.11	0.43	0.09	0.66	0.18
Difference	9.03%	34.3%	25.2%	40.4%	24.94%	58.33%	11.94%	46.21%	

Table 32: Average annual runoff coefficient during the change evaluation period without major climate events before the megadrought onset (1988-2010) and during the megadrought (2010-2020) for the upper and lower sections of each basin. The difference between the two periods relative to 1988-2010 is shown in the third row.

3.3 The impacts of climate and human activities on streamflow

During the complete evaluation period, the near-natural simulated streamflow is higher than the observed streamflow in all the cases (Fig. 6) with mean biases in annual simulated streamflow differences ranging from 65% in the Limarí basin (simulated near-natural annual runoff of 55 mm and observed annual runoff of 36,7 mm) to 30% in the Aconcagua basin (simulated near-natural annual runoff streamflow of 155,4 mm and observed annual runoff of 119,8 mm).

Con formato: Derecha: -0,11"

Con formato: Derecha: -0,11"

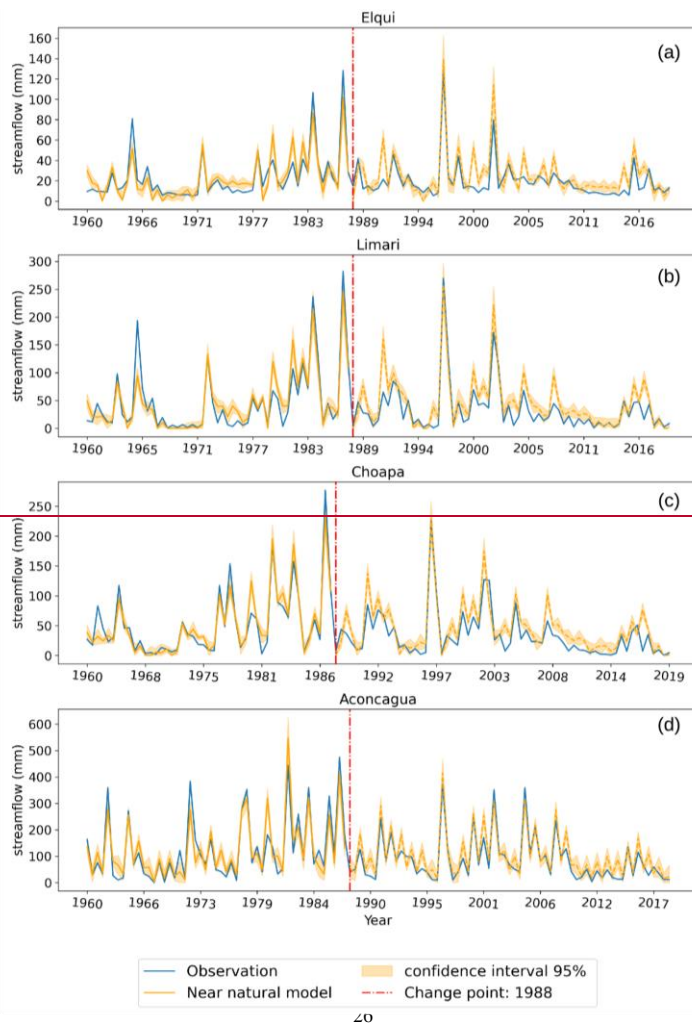
Con formato: Derecha: -0,11"

Con formato: Derecha: -0,11"

Con formato: Izquierda

Con formato: Color de fuente: Automático

Con formato: Borde: Superior: (Sin borde), Inferior: (Sin borde), Izquierda: (Sin borde), Derecha: (Sin borde), Entre : (Sin borde), Punto de tabulación: No en 3,13" 6,27"



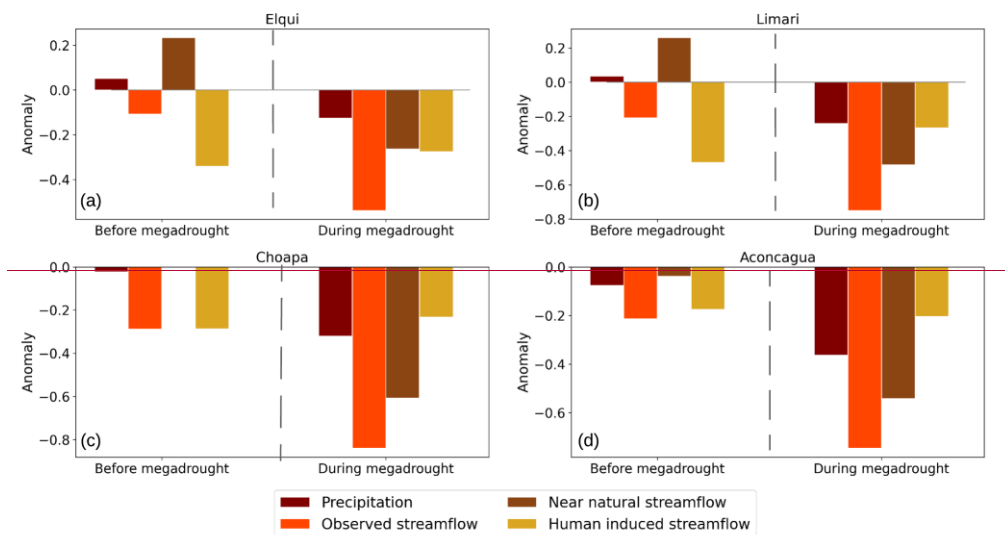
Con formato: Izquierda

Con formato: Color de fuente: Automático

Con formato: Borde: Superior: (Sin borde), Inferior: (Sin borde), Izquierda: (Sin borde), Derecha: (Sin borde), Entre : (Sin borde), Punto de tabulación: No en 3,13" 6,27"

319 **Figure 6.** The observed and near natural simulated seasonal streamflow for Elqui (a), Limari (b), Choapa (c), and Aconcagua (d)
 320 basins, respectively. The continuous yellow line represents the simulated streamflow on the reference period whose r^2 is presented
 321 on the legend. The dashed yellow line is the simulated streamflows on the change period after the breakpoint (red line). the yellow
 322 ban represents the 95% confidence interval.

323 The relative impacts of climate and human activities on summer streamflow reductions during the evaluation period is presented
 324 in Fig. 7. This figure shows the annual anomalies of precipitation, observed and near-natural simulated summer streamflow, as
 325 well as the human-induced streamflow reduction obtained as the difference of the latter two (Eq. 4). The results for the annual
 326 fluxes are presented in Appendix A (Fig. A1).B.



Con formato: Derecha: -0,11"

Con formato: Izquierda

Con formato: Color de fuente: Automático

Con formato: Borde: Superior: (Sin borde), Inferior: (Sin borde), Izquierda: (Sin borde), Derecha: (Sin borde), Entre : (Sin borde), Punto de tabulación: No en 3,13" 6,27"

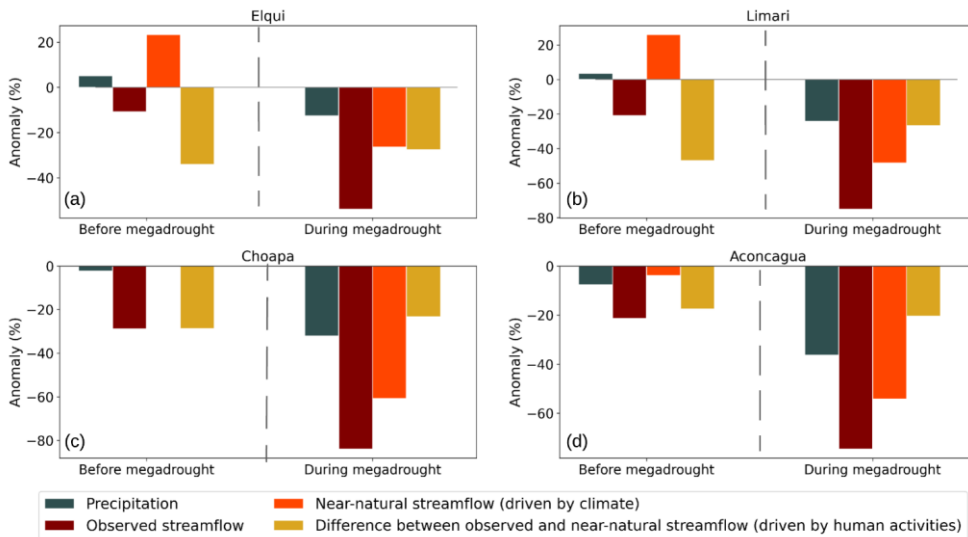


Figure 7: Anomalies in annual precipitation, observed summer streamflow and simulated near-natural summer streamflow, with the derived difference between the latter two, which represent the human-induced streamflow change anomaly for Elqui (a), Limarí (b), Choapa (c), and Aconcagua (d) basins. The anomalies are presented for the evaluation period before and after the megadrought onset (1988-2009 and 2010-2020, respectively). For each flux, the anomalies are computed as the percentage difference with respect to their mean values during the reference period (1960-1988).

Before the megadrought onset, annual precipitation varied between 5 to -7.6% with respect to the 1960-1988 reference period among the study basins. The resulting near-natural summer streamflow during that period followed the direction of the annual precipitation anomalies, with anomalies between 23 to -4% across basins. During that period, the observed summer streamflow -accounting for full climatic and human influences- decreased by 10-28%. This indicates that water uses for human activities were the main driver factor of summer streamflow reduction before the megadrought onset, causing up to 100% of

Con formato: Derecha: -0,11", Espacio Después: 0 p
Borde: Superior: (Sin borde), Inferior: (Sin borde),
Izquierda: (Sin borde), Derecha: (Sin borde), Entre : (S
borde)

Con formato: Derecha: -0,11"

Con formato: Izquierda

Con formato: Color de fuente: Automático

Con formato: Borde: Superior: (Sin borde), Inferior: (Sin
borde), Izquierda: (Sin borde), Derecha: (Sin borde),
Entre : (Sin borde), Punto de tabulación: No en 3,13"
6,27"

339 reduction in Elqui, Limarí and Choapa, and 82% in the Aconcagua Basin, respectively. ~~The human induced decrease on~~
340 ~~Aconcagua accounts for 33.8 mm over the total streamflow deficit of 41.3 mm.~~

341 After the megadrought onset, the relative impact of precipitation deficits and human activities on streamflow depletion changed.
342 The annual precipitation anomalies during the megadrought varied between -13 to -36% across basins, while the near-natural
343 streamflow estimates ~~present~~presented anomalies between -26% to - 61% ~~with respect to the 1960-1988 reference period.%~~.
344 During ~~that~~this period, the observed summer streamflow ~~accounting for full climatic and human influences~~ featured anomalies
345 of -54% to -84%. This ~~indicate~~indicates that precipitation deficits dominate the streamflow ~~reduction~~reductions, however, there
346 is still a relevant reduction ~~of 7.9 mm, 11.9 mm, 15.5mm, and 39.5 mm~~ attributed to human activities, representing 51%, 29%,
347 27%, and 27% of the total summer streamflow reduction in Elqui, Limarí, Choapa, and Aconcagua Basin, respectively.

348 Particularly noteworthy is the Aconcagua basin case, where, in absolute terms, the human induced ~~total~~streamflow reduction
349 during the megadrought (corresponding to an absolute value of 39.5 mm) ~~is~~was higher than ~~is~~during the period before the
350 megadrought (33.8 mm). This has happened despite ~~considerably less the significantly lower~~ water availability (during the
351 megadrought, where near-natural summer streamflow estimates ofwas 88.6 mm during the megadrought and 185.7 mm, which
352 corresponds to less than half of the near-natural summer flow before the megadrought onset (185.7 mm). This apparent
353 contradiction may be attributed to the Aconcagua's increased total water consumption during the megadrought, led by intensified
354 agricultural water demand (Fig. 5a).

355 Consistently with the summer seasons, near-natural annual streamflow before the megadrought followed precipitation patterns,
356 with anomalies between 22 to -5% across basins (Fig. A1). During that period, the observed annual streamflow varied between
357 -2 to -20% across basins. Water uses for human activities were the driver factor of streamflow reduction before the megadrought
358 onset, causing up to 100% of reduction in Elqui, Limarí and Choapa, and 71% in the Aconcagua Basin, respectively. After the
359 megadrought onset, the observed streamflow featured anomalies of -47 to -71%. From these streamflow deficits, a 44% to 75 %
360 of the reduction is attributed to climatic-factors (i.e., anomalies represented by the near-natural simulated streamflow), while the
361 remaining 25 to 56% is attributed to human activities.

Con formato: Izquierda

Con formato: Color de fuente: Automático

Con formato: Borde: Superior: (Sin borde), Inferior: (Sin borde), Izquierda: (Sin borde), Derecha: (Sin borde), Entre : (Sin borde), Punto de tabulación: No en 3,13" 6,27"

3.4 The impacts of human activities on hydrological drought events

The selected hydrological drought events selected based on a seasonal threshold of 80th percentile of the near-natural streamflow (Seet. 2.4) for each basin are shown in Fig. 8. By contrasting the observed and near-natural time series, the climate-induced and human-induced droughts are distinguished. The meteorological megadrought (2010-2020) is identified as a series of associated to several hydrological drought events in, as evidenced by the observed streamflow. In contrast, its time series. However, the megadrought does not seem as to have such a persistent and intense ineffect on the near-natural streamflow scenario.

The largest human impact on hydrological droughts is (computed as the difference between observed in the total seasons in drought and near-natural streamflow drought events) is evident in the total deficit duration and intensity of drought events (Table 43). Elqui, Limari, Choapa, and Aconcagua have 10, 13, 8, 13 and 407 extra seasons of in drought duration, respectively, and more than close to double (triple in Choapa's case) deficit concerning the near-natural scenario. Additionally of streamflow deficits. In general, more drought events (Limari, Choapa and Aconcagua) with a larger average time duration (Elqui and Choapa) and average deficit (Elqui, Choapa and Aconcagua) have occurred in the observed scenario compared to the three basins previously mentioned near-natural scenario. The largest drought event in each basin occurred during the megadrought. Across all basins, the human activities led to an increase in the maximum duration of hydrological droughts, with maximum values ranging between 410 to 4012 seasons, in contrast to 14 to 46 seasons experienced in the near-natural cases. In particular, this translates to five 5 or 6 years of continuous streamflow below the Q80Q70 threshold on the Aconcagua basin.

Basin	Hydrological Droughts	frequency	duration (seasons)			deficit (mm)		
			Total season	Max duration #	Average duration	Total deficit	Max deficit	Average deficit
Elqui	Near-natural	5.0	5.0	1.0	1.0	21.1	10.5	4.2
	Observed	9.0	18.0	9.0	2.0	56.1	29.8	6.2
Limari	Near-natural	3.0	9.0	4.0	3.0	41.4	20.9	13.8
	Observed	6.0	13.0	4.0	2.2	47.5	20.4	7.9
Choapa	Near-natural	5.0	10.0	4.0	2.0	36.1	19.6	7.2
	Observed	6.0	18.0	7.0	3.0	110.1	51.0	18.3
Aconcagua	Near-natural	6.0	14.0	4.0	2.3	337.1	134.5	56.2

Con formato: Izquierda

Con formato: Color de fuente: Automático

Con formato: Borde: Superior: (Sin borde), Inferior: (Sin borde), Izquierda: (Sin borde), Derecha: (Sin borde), Entre : (Sin borde), Punto de tabulación: No en 3,13" 6,27"

379
380
381
382
383
384
385

Observed	10.0	24.0	10.0	2.4	732.0	276.7	73.2
Table 4: during the megadrought. The human influence over hydrological drought varies between the different drought characteristics, but in most cases it causes drought intensification, leading to an increase of 25 to 45% of the total drought events and an increase of 17 to 62% of the total streamflow deficit. The negative percentage difference in mean duration or mean deficit reported for each basin Limari and Aconcagua basins is due to a greater number of short events. However, considering that the total number of events is larger in the observed and simulated near natural streamflow during the evaluation period (1988-2020) scenario, this is not indicative of an alleviation of the drought.							

Con formato: Fuente: 10 pto, Sin Negrita, Color de fuente: Automático

Con formato: Derecha: -0,11", Espacio Después: 0 pto, Borde: Superior: (Sin borde), Inferior: (Sin borde), Izquierda: (Sin borde), Derecha: (Sin borde), Entre : (Sin borde)

Con formato: Fuente: 10 pto, Sin Negrita, Color de fuente: Automático

Con formato: Fuente: 10 pto, Sin Negrita, Color de fuente: Automático

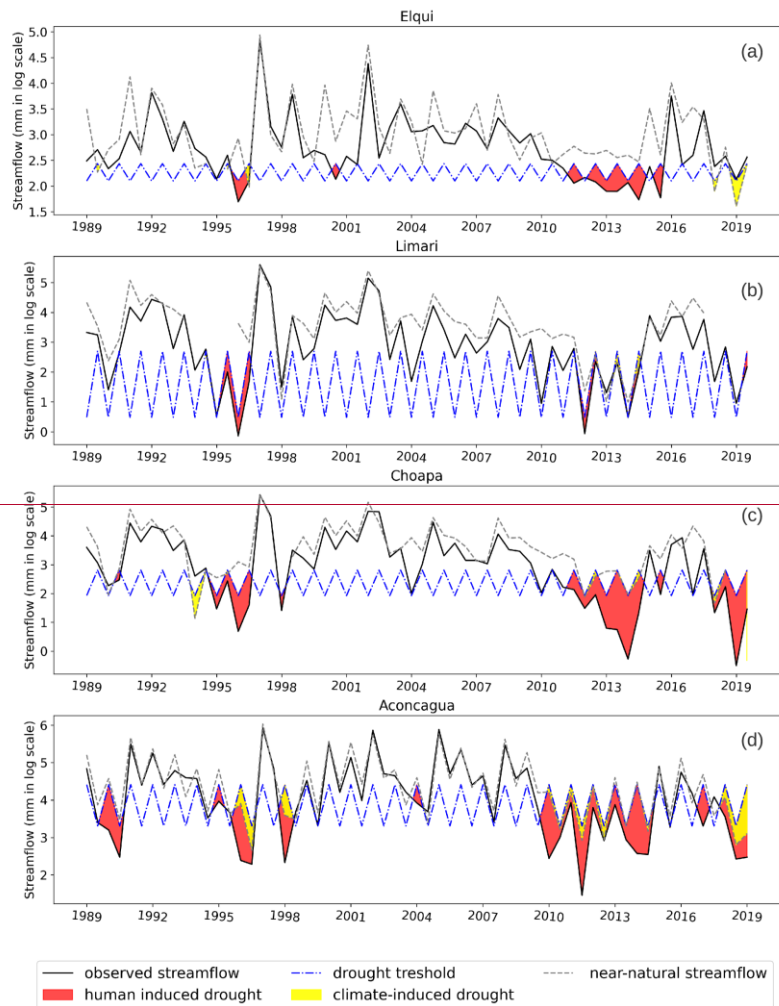
Con formato: Fuente: 10 pto, Sin Negrita, Color de fuente: Automático

Con formato: Fuente: 10 pto, Sin Negrita, Color de fuente: Automático

Con formato: Izquierda

Con formato: Color de fuente: Automático

Con formato: Borde: Superior: (Sin borde), Inferior: (Sin borde), Izquierda: (Sin borde), Derecha: (Sin borde), Entre : (Sin borde), Punto de tabulación: No en 3,13" 6,27"



Con formato: Izquierda

Con formato: Color de fuente: Automático

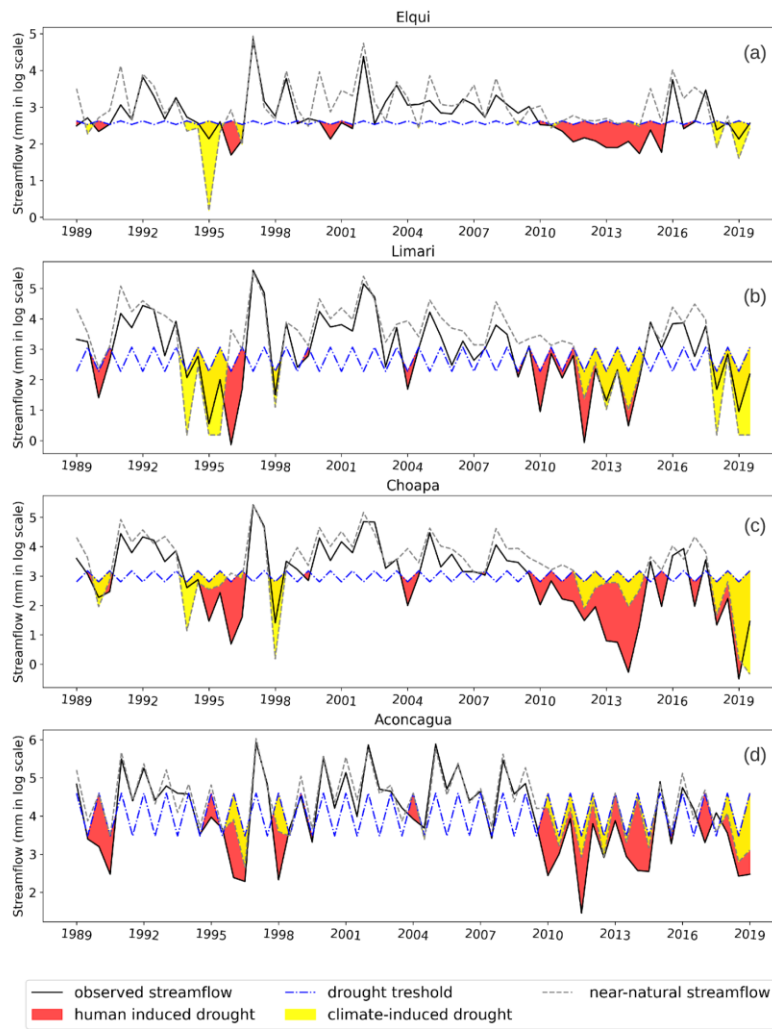
Con formato: Borde: Superior: (Sin borde), Inferior: (Sin borde), Izquierda: (Sin borde), Derecha: (Sin borde), Entre : (Sin borde), Punto de tabulación: No en 3,13" 6,27"

387 When analyzing drought characteristics separately before and during the megadrought (Appendix C), Elqui exhibits a low human
388 impact before the megadrought onset and it notably increases during the megadrought, contributing to 57% of total drought
389 events and nearly 70% of the observed deficit. In contrast, Limari, Choapa, and Aconcagua show a more stable human
390 contribution to drought characteristics before and during the megadrought, with a decrease of human contribution to total events
391 close to 25% (all basins), a decrease in human contribution to total deficit (Limari basin) and a slight increase contribution to
392 total deficit during the megadrought (Choapa basin).

Con formato: Izquierda

Con formato: Color de fuente: Automático

Con formato: Borde: Superior: (Sin borde), Inferior: (Sin borde), Izquierda: (Sin borde), Derecha: (Sin borde), Entre : (Sin borde), Punto de tabulación: No en 3,13" 6,27"



Con formato: Izquierda

Con formato: Color de fuente: Automático

Con formato: Borde: Superior: (Sin borde), Inferior: (Sin borde), Izquierda: (Sin borde), Derecha: (Sin borde), Entre : (Sin borde), Punto de tabulación: No en 3,13" 6,27"

394 **Figure 8. Observed and near-natural streamflow and hydrological drought events during the evaluation period (1988–2020) for Elqui**
 395 **(a), Limarí (b), Choapa (c), and Aconcagua (d) basins, respectively.**

Basin	Hydrological Drought	frequency	duration (seasons)			deficit (mm)		
			Total season	Max duration	Total season	Max duration	Total season	Max duration
Elqui	Near- natural	10.00	16.00	4.00	1.60	51.61	20.55	5.16
	Observed	10.00	26.00	12.00	2.60	95.30	54.77	9.53
	diff %	0.00%	38.46%	66.67%	38.46%	45.84%	62.47%	45.84%
Limarí	Near- natural	5.00	16.00	6.00	3.20	157.34	51.69	31.47
	Observed	10.00	29.00	10.00	2.90	191.62	77.05	19.16
	diff %	50.00%	44.83%	40.00%	-10.34%	17.89%	32.92%	-64.22%
Choapa	Near- natural	7.00	19.00	6.00	2.71	181.43	58.31	25.92
	Observed	11.00	32.00	11.00	2.91	355.70	142.27	32.34
	diff %	36.36%	40.63%	45.45%	6.70%	48.99%	59.01%	19.85%
Aconcagua	Near- natural	7.00	20.00	6.00	2.86	411.97	133.27	58.85
	Observed	12.00	27.00	10.00	2.25	1074.65	415.00	89.55
	diff %	41.67%	25.93%	40.00%	-26.98%	61.66%	67.89%	34.28%

397 **Table 3: drought characteristics for each basin considering the observed and simulated near natural streamflow during the evaluation**
 398 **period (1988-2020). The third row for each basin represents the human influence on drought characteristics as the percentage**
 399 **difference between the observed and the naturalized scenario**

400 **4 Discussion**

401 **4.1 Impact of increased human activities on water availability**

402 During the megadrought, precipitation deficits have played a more significant role on the decrease in annual streamflow than
 403 anthropogenicanthropic factors, however, human activities still account for approximately 27 to 29% of the streamflow reduction
 404 in the Aconcagua, Choapa, and Limarí basins and 51% in Elqui, the basin least affected by the meteorological megadrought.

405 Human activities have intensified since the 1980s and 1990s, driven by rising water demand from economic activities,
 406 population growth, and land use changes (Fig. 5a), despite the precipitation deficits and streamflow reduction during the

Con formato: Color de fuente: Negro

Con formato: Derecha: -0,11", Borde: Superior: (Sin borde), Inferior: (Sin borde), Izquierda: (Sin borde), Derecha: (Sin borde), Entre : (Sin borde)

Con formato: Color de fuente: Negro

Con formato: Color de fuente: Negro

Con formato: Color de fuente: Negro

Con formato: Color de fuente: Negro

Con formato: Derecha: -0,11"

Con formato: Izquierda

Con formato: Color de fuente: Automático

Con formato: Borde: Superior: (Sin borde), Inferior: (Sin borde), Izquierda: (Sin borde), Derecha: (Sin borde), Entre : (Sin borde), Punto de tabulación: No en 3,13", 6,27"

407 megadrought. This suggest that total water consumption has been inelastic to the surface water deficits. In the Aconcagua
408 basin, the total water consumption increased during the megadrought, while in the other three basins, the human induced
409 streamflow reduction expressed as mm is slightly smaller during the megadrought, compared to the period prior to the
410 megadrought (Fig. 7). This finding could be explained by an initial reduction in agricultural water consumption during the first
411 years of the megadrought, which was later reversed (Fig. 5a) by higher extractions of groundwater sources in the subsequent
412 years (Taucare et al., 2020; Duran-Llacer et al., 2020).

413 Human activities have intensified since the 1980s, driven by rising water demand from economic activities, population growth,
414 and land use changes (Fig. 5a), despite the precipitation deficits and streamflow reduction during the megadrought. In general,
415 the basins with the greatest increases in total water consumption during the evaluation period also exhibit higher human influence
416 in the reduction of streamflow. Elqui and Limari exhibited the most significant relative increase in total water consumption,
417 primarily driven by a substantial rise in agriculture consumption from 1989 to 2010, while Choapa almost duplicated its total
418 water consumption during the 2000-2010 decade due to mining operations. It is noteworthy that agriculture and mining water
419 consumption continued to rise during the megadrought.

420 This suggests that total water consumption from surface and groundwater sources has been somehow inelastic to the surface
421 water deficits. In the Aconcagua basin, the human-induced streamflow reduction expressed as mm increased during the
422 megadrought, while in the other three basins was slightly smaller compared to the period prior to the megadrought (Fig. 7). This
423 finding can be explained by an initial reduction in agricultural water consumption during the first years of the megadrought,
424 which was later reversed (Fig. 5a) by higher extractions of groundwater sources in the subsequent years (Taucare et al., 2020;
425 Duran-Llacer et al., 2020).

426 Groundwater sources play a crucial role in streamflow within this study region, and the declines of groundwater levels caused
427 by meteorological droughts and water extractions have critical impacts on water accessibility in rural areas (Crespo et al., 2020;
428 Taucare et al., 2020; Alvarez-Garretón et al., 2021; 2023a; 2023b). These declines can also lead to the disconnection between
429 surface and underground water sources, leading to a decrease in soil moisture conditions (agricultural drought) and the
430 desiccation of rivers and lakes (Duran-Llacer et al., 2022; Muñoz et al., 2020). This exacerbates hydrological drought, delaying
431 the recovery of catchments from drought episodes. Also, irrigation water extraction shifts from surface to groundwater sources,
432 intended to alleviate megadrought impacts, also promotes the inelastic behaviour of water consumption rates. In fact, new surface

Con formato: Izquierda

Con formato: Color de fuente: Automático

Con formato: Borde: Superior: (Sin borde), Inferior: (Sin
borde), Izquierda: (Sin borde), Derecha: (Sin borde),
Entre : (Sin borde), Punto de tabulación: No en 3,13"
6,27"

433 and underground water use rights have been granted during the megadrought (Barría et al., 2021b). This has led to increases in
434 water stress levels and reduction of groundwater reservoirs, which could ultimately lead to an absolute day zero (Alvarez-
435 Garreton et al., 2023b).

436 Human activities account for approximately 25% of the reduction in streamflow during the evaluation megadrought period in
437 most basins, and their effects on hydrological droughts have been significant. Despite experiencing lower precipitation deficits,
438 the Elqui basin shows a similar pattern of hydrological drought recurrence, total seasons, and maximum duration compared to
439 the Choapa and Aconcagua other basins. During the megadrought, this the Elqui basin was the most affected by increased human
440 activities, with the number a 57% of drought seasons increasing from 5 in the near-natural scenario being attributable to 18 in the
441 observed data human contributions to streamflow reduction. This suggests that increased and inelastic human water demands are
442 particularly relevant in semi-arid basins with limited precipitation and high interannual variability in terms of precipitation
443 regime, such as Elqui, making them. This makes highly intervened basins in semi-arid regions more prone to experience a more
444 severe hydrological drought during precipitation deficits. This is consistent with Huang (2016), who highlighted that sustainable
445 agricultural development is threatened in arid and semi-arid regions due to limited available water resources, and with Saft et al.
446 (2016), who demonstrated that aridity is a crucial factor influencing streamflow sensitivity to interdecadal climate variability.

447 **4.2 Drought vulnerability**

448 Hydrological drought vulnerability is associated with those conditions that cause an increase in the frequency, duration, and
449 intensity of the hydrological droughts when a precipitation deficit threat is faced. Vulnerability should be addressed by looking
450 for sensitivity variables that come from the biophysical basin's characteristics, such as aridity, location, geomorphology,
451 hydrological regime, natural land cover, and snow and glacier cover (Saft et al., 2015; Van Loon and Laaha, 2015), and human
452 activities such as management and extraction of water, land use, land cover changes, urbanisation, between others (Barría et
453 al., 2021a; Van Loon et al., 2016, 2022). Although several articles have assessed hydrological drought vulnerability by
454 evaluating biophysical basin characteristics (Alvarez-Garreton et al., 2021; Van Loon and Laaha, 2015; Saft et al., 2015; Van
455 Lanen et al., 2013), there is still a gap in understanding how human activities contribute to basin's vulnerability to drought.

456 As discussed in Sect. 4.1, human activities have intensified streamflow deficits during the megadrought. Although our results
457 correspond to four basins in central Chile, the large streamflow deficits have been reported over a wider region, with a range
458 of impacts on society and ecosystems. For example, (Miranda et al., 2020) reported that water courses stopped flowing at

Con formato: Derecha: -0,11"

Con formato: Izquierda

Con formato: Color de fuente: Automático

Con formato: Borde: Superior: (Sin borde), Inferior: (Sin borde), Izquierda: (Sin borde), Derecha: (Sin borde), Entre : (Sin borde), Punto de tabulación: No en 3,13" 6,27"

459 certain periods of the year during the megadrought, while a significant effect has been observed on forest productivity with
460 high tree mortality. Additionally, thousands of people have lost access to domestic water services (Muñoz et al., 2020).
461 National statistics indicate that spending on cistern trucks to deliver potable water to rural communities in the six main
462 watersheds of Coquimbo and Valparaíso regions reached US\$56 million during 2010–2020. Human activities that affect
463 catchment vulnerability in central Chile include groundwater extractions (Taucare et al., 2020), overallocation of water use
464 rights (Alvarez Garreton et al., 2021; Barría et al., 2021a), and continuous land use change for agricultural purposes
465 (Madariaga et al., 2021). For example, agriculture is sometimes established on hillsides with high slopes, exacerbating water
466 consumption problems and changing runoff mechanisms. In the entire Aconcagua basin, the water consumption of avocado
467 plantations has increased 15% between 2014 and 2020, reaching almost 4.8 M3/s, while citrus plantations have increased 67–
468 70% in the Elqui and Limarí basins since 2010, reaching 1.8 M3/s of water consumption in the Limarí basin. This reveals that
469 water use for agriculture activities has been inelastic to the precipitation deficits during the megadrought. Human activities in
470 these basins are adapting to less water availability in ways that are leading to aggravated water scarcity problems, which is
471 consider in the literature as maladaptation (Schipper, 2020).

472 **4.2 Drought vulnerability**

473 Hydrological drought vulnerability is associated with those conditions that cause an increase in the frequency, duration, and
474 intensity of the hydrological droughts when a precipitation deficit threat is faced. Vulnerability should be addressed by looking
475 for sensitivity variables that come from the biophysical basin's characteristics, such as aridity, location, geomorphology,
476 hydrological regime, natural land cover, and snow and glacier cover (Saft et al., 2015; Van Loon and Laaha, 2015), and human
477 activities such as management and extraction of water, land use, land cover changes, urbanisation, between others (Barría et al.,
478 2021a; Van Loon et al., 2016, 2022).

479 As discussed in Sect. 4.1, human activities have intensified streamflow deficits during the megadrought. Human activities that
480 affect catchment vulnerability in central Chile include groundwater extractions (Taucare et al., 2020), overallocation of water
481 use rights (Alvarez-Garreton et al., 2021; Barría et al., 2021a), and continuous land use change for agricultural purposes
482 (Madariaga et al., 2021). For example, agriculture is sometimes established on hillsides with high slopes, exacerbating water
483 consumption problems and changing runoff mechanisms. In the entire Aconcagua basin, the water consumption of avocado
484 plantations has increased 15% between 2014 and 2020, reaching almost 4.8 m³/s, while citrus plantations have increased 67-
485 70% in the Elqui and Limarí basins since 2010, reaching 1.8 m³/s of water consumption in the Limarí basin. This reveals that

Con formato: Izquierda

Con formato: Color de fuente: Automático

Con formato: Borde: Superior: (Sin borde), Inferior: (Sin borde), Izquierda: (Sin borde), Derecha: (Sin borde), Entre : (Sin borde), Punto de tabulación: No en 3,13" 6,27"

486 irrigated agriculture has been inelastic to the precipitation deficits during the megadrought. Human activities in these basins are
487 adapting to less water availability in ways that are leading to aggravated water scarcity problems, which is considered in the
488 literature as maladaptation (Schipper, 2020).

489 Precipitation deficits and human activities including human-induced maladaptation processes have broad, complex and
490 exacerbated impacts on society and ecosystems. For example, agricultural practices may worsen water scarcity problems and
491 contribute to soil erosion and sediment transport (Owens, 2020), further degrading ecosystem health. The intensified streamflow
492 deficits have disrupted watercourses and contribute to tree mortality (Miranda et al., 2020). Additionally, thousands of people
493 have lost access to domestic water services (Muñoz et al., 2020), leading to a large spending on water cistern trucks (Alvarez-
494 Garreton et al., 2023a). These impacts reveal that there is still a gap in understanding how human activities contribute to
495 catchment vulnerability to hydrological droughts and how their influence on the hydrological cycle can be effectively included
496 in drought management (Anne F. Van Loon et al., 2016). In the case of Chile, previous studies have shown that the current water
497 management policy inadequately addresses the physical constraints of surface and groundwater availability, contributing to an
498 inadequate prevention of water stress conditions (Alvarez-Garreton et al., 2023a). This calls for urgent modifications in the water
499 management system to ensure sustainable water use and prevent the exacerbation of water stress conditions in the region.

500 **4.3 Study limitations**

501 Our approach and insights are based on attribution exercises that compare the observed streamflow and a naturalised simulation
502 of it, which permits to isolate the effect of human activities. In this study, the near-natural simulation was done by using
503 regression statistical methods, which have limitations that should be considered: they do not explicitly account for the physical
504 mechanisms of runoff generation, they rely solely on precipitation as a predictor and they consider a linear relationship between
505 the variables. Although the attribution exercise is still consistent, this methodological limitation prevents to drawing
506 conclusions regarding the physical mechanisms involved in streamflow reduction during droughts. To enable a physical
507 interpretation, and likely a better representation of streamflow generation and memory effects, future studies should advance
508 into implementing physically-based models to performed the attribution exercises.

509 Independently of the adopted model, the streamflow estimations have uncertainties that can mask some of the human influence
510 effects in the attribution exercise. In order to visualize this potential artefact, Fig. 6 shows the streamflow estimations with a
511 95% confidence interval. These plots, in general, show that the lowest values of naturalized streamflow are above the observed

Con formato: Izquierda

Con formato: Color de fuente: Automático

Con formato: Borde: Superior: (Sin borde), Inferior: (Sin borde), Izquierda: (Sin borde), Derecha: (Sin borde), Entre : (Sin borde), Punto de tabulación: No en 3,13" 6,27"

512 time series. Anyway, considering the lower performance of the winter models in some catchments and that the summer season
513 concentrates most human intervention due to agricultural activities, we have primarily focused on exploring the results of this
514 season (Fig. 7).

515 Considering the evidence of potential climate-driven non-stationarities on streamflow generation during the megadrought in
516 Chilean catchments (Alvarez-Garreton et al., 2021), the attribution of human activities as the driving factor of the intensified
517 streamflow reduction should then interpreted carefully. The intensification in streamflow reduction is attributed to the
518 combination of human activities, natural hydrological processes, and the potential effects of non-stationarity catchment
519 response. Since the upper catchment sections have a lower human influence (but still influenced) than the downstream sections,
520 the larger streamflow decrease during the megadrought (compared to the previous period) in these sections may be mostly (but
521 not fully) attributed to non-stationarity in basin response during protracted droughts (consistent with Saft et al., 2015; Alvarez-
522 Garreton et al., 2021). However, the downstream sections feature an even larger streamflow reduction during the megadrought
523 compared to the reduction in the upper sections (Table 2). This is consistent to the added effect of human activities on
524 streamflow reduction, which have maintained water consumption despite the reduced water availability (Fig. 5).

525 **5 Conclusions**

526 The megadrought in central Chile ~~corresponds to~~has been the longest dry period over the last centuries. The study basins featured
527 a range of 16-~~to~~ 41% in mean annual precipitation deficits during this period, whereas the deficits in observed streamflow were
528 significantly larger. The Elqui, Limarí, Choapa, and Aconcagua Basin experienced deficits in summer streamflow of 54%, 75%,
529 84%, and 75%, respectively.

530 Our findings indicate that human activities were the main driving factor of streamflow reduction before the megadrought began
531 in 2010-onset. During the megadrought, human activities still accounted for a significant portion of streamflow reduction,
532 ranging from 27 to 51%. The impact of human activities on hydrological drought characteristics was substantial, leading to more
533 than double the recurrence, duration, and intensity of droughts in some basins. ~~Furthermore, our results show that human~~
534 ~~activities have dominated the decline of the rainfall-runoff ratios during the megadrought in the study basins.~~

535 ~~Human activities in these basins show limited adaptation to the decreasing water availability. During the megadrought, new~~
536 ~~surface and underground water use rights have been granted (Barría et al., 2021b). Human activities in these basins have shown~~

Con formato: Derecha: -0,11"

Con formato: Izquierda

Con formato: Color de fuente: Automático

Con formato: Borde: Superior: (Sin borde), Inferior: (Sin borde), Izquierda: (Sin borde), Derecha: (Sin borde), Entre : (Sin borde), Punto de tabulación: No en 3,13" 6,27"

537 [limited adaptation to the decrease in water availability](#). The increase in human water demand, often inelastic to the decreased
538 surface water availability, makes basins more vulnerable to severe hydrological droughts when precipitation deficits are faced,
539 especially on semi-arid basins with water availability constraints.

540 This paper demonstrates that during long and persistent dry periods, human activities within the catchment strongly influence
541 the intensity and duration of hydrological drought. To effectively adapt to climate change and avoid maladaptation measures, it
542 is necessary to consider the feedback between water use, [anthropogenic](#) activity, and the hydrological system. These
543 considerations are particularly important in Chile and other territories [around the world](#), where the dry signal is
544 consistent and expected to persist.

545 **Data availability**

546 The CR2MET dataset were obtained from the Center for Climate and Resilience Research website at [https://www.cr2.cl/datos-](https://www.cr2.cl/datos-productos-grillados)
547 [productos-grillados](https://www.cr2.cl/datos-productos-grillados) (last access: 20 September 2023). The water use data was
548 obtained upon request from the Center for Climate and Resilience Research website at
549 <https://seguridadhidrica.cr2.cl> (last access: 20 September 2023). The streamflow data were
550 obtained from CAMELS-CL dataset (Alvarez-Garreton et al., 2018), available at the Center for Climate and Resilience
551 Research website at <https://camels.cr2.cl> (last access: 20 September 2023).

552 **Author contributions**

553 NA, CAG and AM conceived the idea of the research. NA performed the analyses. NA and CAG wrote much of the manuscript.
554 All the authors reviewed early manuscript drafts and the final draft.

555 **Competing interests**

556 The contact author has declared that none of the authors has any competing interests.

Con formato: Inglés (Reino Unido)

Con formato: Inglés (Reino Unido)

Con formato: Inglés (Reino Unido)

Con formato: Inglés (Reino Unido)

Con formato: Inglés (Reino Unido)

Con formato: Inglés (Reino Unido)

Con formato: Izquierda

Con formato: Color de fuente: Automático

Con formato: Borde: Superior: (Sin borde), Inferior: (Sin borde), Izquierda: (Sin borde), Derecha: (Sin borde), Entre : (Sin borde), Punto de tabulación: No en 3,13" 6,27"

557 **Acknowledgements:**

558 This research has been developed within the framework of the Center for Climate and Resilience Research (CR2,
559 ANID/FONDAP/1522A0001), the research project ANID/FSEQ210001, [ANID/FONDECYT/1201714](#) and
560 ANID/FONDECYT/[120171411240924](#).

561 **References**

- 562 Alvarez-Garretón, C., Mendoza, P. A., Pablo Boisier, J., Addor, N., Galleguillos, M., Zambrano-Bigiarini, M., Lara, A., Puelma,
563 C., Cortes, G., Garreaud, R., McPhee, J., and Ayala, A.: The CAMELS-CL dataset: Catchment attributes and meteorology
564 for large sample studies-Chile dataset, *Hydrol. Earth Syst. Sci.*, 22, 5817–5846, <https://doi.org/10.5194/hess-22-5817-2018>,
565 2018.
- 566 Alvarez-Garretón, C., Pablo Boisier, J., Garreaud, R., Seibert, J., and Vis, M.: Progressive water deficits during multiyear
567 droughts in basins with long hydrological memory in Chile, *Hydrol. Earth Syst. Sci.*, 25, 429–446,
568 <https://doi.org/10.5194/hess-25-429-2021>, 2021.
- 569 Alvarez-Garretón, C., Boisier, J.P., Blanco, G., Billi, M., Nicolas-Artero, C., Maillet, A., Aldunce, P., Urrutia-Jalabert, R.,
570 Zambrano-Bigiarini, M., Guevara, G., Galleguillos, M., Muñoz, A., Christie, D., Marinao, R., & Garreaud, R.: *Seguridad*
571 *Hídrica en Chile: Caracterización y Perspectivas de Futuro*. Centro de Ciencia del Clima y la Resiliencia CR2,
572 (ANID/FONDAP/1522A0001), 72 pp. Disponible en www.cr2.cl/seguridadhidrica, 2023a
- 573 Alvarez-Garretón, C., Boisier, J. P., Garreaud, R., González, J., Rondanelli, R., Gayó, E., and Zambrano-Bigiarini, M.: HESS
574 Opinions: The unsustainable use of groundwater conceals a “Day Zero”, *Hydrol. Earth Syst. Sci. Discuss.* [preprint],
575 <https://doi.org/10.5194/hess-2023-245>, in review, 2023b.
- 576 Barría, P., Sandoval, I. B., Guzman, C., Chadwick, C., Alvarez-Garretón, C., Díaz-Vasconcellos, R., Ocampo-Melgar, A., and
577 Fuster, R.: Water allocation under climate change: A diagnosis of the Chilean system, *Elementa*, 9, 1–20,
578 <https://doi.org/10.1525/elementa.2020.00131>, 2021a.
- 579 Barría, P., Chadwick, C., Ocampo-Melgar, A., Galleguillos, M., Garreaud, R., Díaz-Vasconcellos, R., Poblete, D., Rubio-
580 Álvarez, E., and Poblete-Caballero, D.: Water management or megadrought: what caused the Chilean Aculeo Lake drying?,
581 <https://doi.org/10.1007/s10113-021-01750-w>, 2021b.
- 582 Boisier, J. P., Alvarez-Garretón, C., Cordero, R. R., Damiani, A., Gallardo, L., Garreaud, R. D., Lambert, F., Ramallo, C., Rojas,

Con formato: Inglés (Reino Unido)

Con formato: Izquierda

Con formato: Color de fuente: Automático

Con formato: Borde: Superior: (Sin borde), Inferior: (Sin borde), Izquierda: (Sin borde), Derecha: (Sin borde), Entre : (Sin borde), Punto de tabulación: No en 3,13" 6,27"

583 M., and Rondanelli, R.: Anthropogenic drying in central-southern Chile evidenced by long-term observations and climate
584 model simulations, *Elementa*, 6, 74, <https://doi.org/10.1525/elementa.328>, 2018.

585 Bozkurt, D., Rojas, M., Boisier, J. P., and Valdivieso, J.: Climate change impacts on hydroclimatic regimes and extremes over
586 Andean basins in central Chile, *Hydrol. Earth Syst. Sci. Discuss.*, 17, 1–29, <https://doi.org/10.5194/hess-2016-690>, 2017.

587 Budds, J.: La demanda, evaluación y asignación del agua en el contexto de escasez, *Rev. Geogr. Norte Gd.*, 52, 167–184, 2012.

588 Buishand, T. A.: Some methods for testing the homogeneity of rainfall records, *J. Hydrol.*, 58, 11–27,
589 [https://doi.org/10.1016/0022-1694\(82\)90066-X](https://doi.org/10.1016/0022-1694(82)90066-X), 1982.

590 Chiew, F. H. S., Peel, M. C., McMahon, T. A., and Siriwardena, L. W.: Precipitation elasticity of streamflow in catchments
591 across the world, *IAHS-AISH Publ.*, 256–262, <https://doi.org/10.3390/w12092446> 2006.

592 Crespo, S. A., Lavergne, C., Fernandoy, F., Muñoz, A. A., Cara, L., and Olfos-Vargas, S.: Where does the Chilean Aconcagua
593 river come from? Use of natural tracers for water genesis characterization in glacial and periglacial environments, *Water*
594 (Switzerland), 12, <https://doi.org/10.3390/w12092630>, 2020.

595 CR2MET: A high-resolution precipitation and temperature dataset for the period 1960–2021 in continental Chile:
596 <https://doi.org/10.5281/zenodo.7529682>, last access: 10 December 2022.

597

598 Duran-Llacer, I., Munizaga, J., Arumí, J. L., Ruybal, C., Aguayo, M., Sáez-Carrillo, K., Arriagada, L., and Rojas, O.: Lessons
599 to be learned: Groundwater depletion in Chile's Ligüa and Petorca watersheds through an interdisciplinary approach, *Water*
600 (Switzerland), 12, <https://doi.org/10.3390/w12092446>, 2020.

601 Esri. "Topographic" [basemap]. Scale Not Given. "World Topographic Map". 2017.
602 <https://www.arcgis.com/home/item.html?id=7dc6cea0b1764a1f9af2e679f642f0f5>. (October 24, 2023).

603 Fleig, A. K., Tallaksen, L. M., Hisdal, H., Stahl, K., and Hannah, D. M.: Inter-comparison of weather and circulation type
604 classifications for hydrological drought development, *Phys. Chem. Earth*, 35, 507–515,
605 <https://doi.org/10.1016/j.pce.2009.11.005>, 2010.

606 Garreaud, R., Alvarez-Garreton, C., Barichivich, J., Pablo Boisier, J., Christie, D., Galleguillos, M., LeQuesne, C., McPhee, J.,
607 and Zambrano-Bigiarini, M.: The 2010–2015 megadrought in central Chile: Impacts on regional hydroclimate and vegetation,
608 *Hydrol. Earth Syst. Sci.*, 21, 6307–6327, <https://doi.org/10.5194/hess-21-6307-2017>, 2017.

609 Garreaud, R., Boisier, J. P., Rondanelli, R., Montecinos, A., Sepúlveda, H. H., and Veloso-Aguila, D.: The Central Chile Mega
610 Drought (2010–2018): A climate dynamics perspective, *Int. J. Climatol.*, 40, 421–439, <https://doi.org/10.1002/joc.6219>,
611 2020.

Con formato: Izquierda

Con formato: Color de fuente: Automático

Con formato: Borde: Superior: (Sin borde), Inferior: (Sin
borde), Izquierda: (Sin borde), Derecha: (Sin borde),
Entre : (Sin borde), Punto de tabulación: No en 3,13"
6,27"

- 612 González-Reyes, Á., McPhee, J., Christie, D. A., Quesne, C. Le, Szejner, P., Masiokas, M. H., Villalba, R., Muñoz, A. A., and
613 Crespo, S.: Spatiotemporal variations in hydroclimate across the Mediterranean Andes (30°-37°S) since the early twentieth
614 century, *J. Hydrometeorol.*, 18, 1929–1942, <https://doi.org/10.1175/JHM-D-16-0004.1>, 2017.
- 615 González-Reyes, Á., Jacques-Coper, M., Bravo, C., Rojas, M., and Garreaud, R.: Evolution of heatwaves in Chile since 1980,
616 *Weather Clim. Extrem.*, 41, 100588, <https://doi.org/10.1016/j.wace.2023.100588>, 2023.
- 617 Huang, S., Liu, D., Huang, Q., and Chen, Y.: Contributions of climate variability and human activities to the variation of runoff
618 in the Wei River Basin, China, *Hydrol. Sci. J.*, 61, 1026–1039, <https://doi.org/10.1080/02626667.2014.959955>, 2016.
- 619 Jacques-Coper, M. and Garreaud, R. D.: Characterization of the 1970s climate shift in South America, *Int. J. Climatol.*, 35,
620 2164–2179, <https://doi.org/10.1002/joc.4120>, 2015.
- 621 Kayano, M., de Oliveira, C., and Andreoli, R.: Interannual relations between South American rainfall and tropical sea surface
622 temperature anomalies before and after 1976, *Int. J. Climatol.*, 29, <https://doi.org/10.1002/joc.1824>, 2009.
- 623 Kingston, D. G., Stagge, J. H., Tallaksen, L. M., and Hannah, D. M.: European-scale drought: Understanding connections
624 between atmospheric circulation and meteorological drought indices, *J. Clim.*, 28, 505–516, <https://doi.org/10.1175/JCLI-D-14-00001.1>, 2015.
- 625
- 626 Kong, D., Miao, C., Wu, J., and Duan, Q.: Impact assessment of climate change and human activities on net runoff in the Yellow
627 River Basin from 1951 to 2012, *Ecol. Eng.*, 91, 566–573, <https://doi.org/10.1016/j.ecoleng.2016.02.023>, 2016.
- 628 Li, J., Xie, S. P., Cook, E. R., Chen, F., Shi, J., Zhang, D. D., Fang, K., Gou, X., Li, T., Peng, J., Shi, S., and Zhao, Y.: Deciphering
629 Human Contributions to Yellow River Flow Reductions and Downstream Drying Using Centuries-Long Tree Ring Records,
630 *Geophys. Res. Lett.*, 46, 898–905, <https://doi.org/10.1029/2018GL081090>, 2019.
- 631 Linton, J. and Budds, J.: The hydrosocial cycle: Defining and mobilizing a relational-dialectical approach to water, *Geoforum*,
632 57, 170–180, <https://doi.org/10.1016/j.geoforum.2013.10.008>, 2014.
- 633 Liu, Y., Ren, L., Zhu, Y., Yang, X., Yuan, F., Jiang, S., and Ma, M.: Evolution of Hydrological Drought in Human Disturbed
634 Areas: A Case Study in the Laohahe Catchment, Northern China, *Adv. Meteorol.*, 2016,
635 <https://doi.org/10.1155/2016/5102568>, 2016.
- 636 Madariaga, A., Maillet, A., and Rozas, J.: Multilevel business power in environmental politics: the avocado boom and water
637 scarcity in Chile, *Env. Polit.*, 30, 1174–1195, <https://doi.org/10.1080/09644016.2021.1892981>, 2021.
- 638 Miranda, A., Lara, A., Altamirano, A., Di Bella, C., González, M. E., and Julio Camarero, J.: Forest browning trends in response
639 to drought in a highly threatened mediterranean landscape of South America, *Ecol. Indic.*, 115, 106401,
640 <https://doi.org/10.1016/j.ecolind.2020.106401>, 2020.

Con formato: Izquierda

Con formato: Color de fuente: Automático

Con formato: Borde: Superior: (Sin borde), Inferior: (Sin borde), Izquierda: (Sin borde), Derecha: (Sin borde), Entre : (Sin borde), Punto de tabulación: No en 3,13" 6,27"

641 Muñoz-Sabater, J., Dutra, E., Agustí-Panareda, A., Albergel, C., Arduini, G., Balsamo, G., Boussetta, S., Choulga, M., Harrigan,
642 S., Hersbach, H., Martens, B., Miralles, D. G., Piles, M., Rodríguez-Fernández, N. J., Zsoter, E., Buontempo, C., and Thépaut,
643 J. N.: ERA5-Land: A state-of-the-art global reanalysis dataset for land applications, *Earth Syst. Sci. Data*, 13, 4349–4383,
644 <https://doi.org/10.5194/essd-13-4349-2021>, 2021.

645 Muñoz, A. A., Klock-Barría, K., Alvarez-Garreton, C., Aguilera-Betti, I., González-Reyes, Á., Lastra, J. A., Chávez, R. O.,
646 Barría, P., Christie, D., Rojas-Badilla, M., and Lequesne, C.: Water crisis in petorca basin, Chile: The combined effects of a
647 mega-drought and water management, *Water (Switzerland)*, 12, <https://doi.org/10.3390/w12030648>, 2020.

648 Owens, P. N.: Soil erosion and sediment dynamics in the Anthropocene: a review of human impacts during a period of rapid
649 global environmental change, *J. Soils Sediments*, 20, 4115–4143, <https://doi.org/10.1007/s11368-020-02815-9>, 2020.

650 Rangoecroft, S., Van Loon, A. F., Maureira, H., Verbist, K., and Hannah, D. M.: An observation-based method to quantify the
651 human influence on hydrological drought: upstream–downstream comparison, *Hydrol. Sci. J.*, 64, 276–287,
652 <https://doi.org/10.1080/02626667.2019.1581365>, 2019.

653 Rodionov, S. N.: A sequential algorithm for testing climate regime shifts, *Geophys. Res. Lett.*, 31, 2–5,
654 <https://doi.org/10.1029/2004GL019448>, 2004.

655 Saft, M., Western, A. W., Zhang, L., Peel, M. C., and Potter, N. J.: The influence of multiyear drought on the annual rainfall-
656 runoff relationship: An Australian perspective, *Water Resour. Res.*, 51, 2444–2463, <https://doi.org/10.1002/2014WR015348>,
657 2015.

658 Schipper, E. L. F.: Maladaptation: When Adaptation to Climate Change Goes Very Wrong, *One Earth*, 3, 409–414,
659 <https://doi.org/10.1016/j.oneear.2020.09.014>, 2020.

660 Sharifi, A., Mirabbasi, R., Ali Nasr-Esfahani, M., Torabi Haghighi, A., and Fatahi Nafchi, R.: Quantify the impacts of
661 anthropogenic changes and climate variability on runoff changes in central plateau of Iran using nine methods, *J. Hydrol.*,
662 603, 127045, <https://doi.org/10.1016/j.jhydrol.2021.127045>, 2021.

663 Shourov, M. M. H.: mmhs013/pyHomogeneity: tag for Zenodo Release, <https://doi.org/10.5281/ZENODO.3785287>, 2020.

664 Taucare, M., Daniele, L., Viguier, B., Vallejos, A., and Arancibia, G.: Groundwater resources and recharge processes in the
665 Western Andean Front of Central Chile, *Sci. Total Environ.*, 722, 137824, <https://doi.org/10.1016/j.scitotenv.2020.137824>,
666 2020.

667 Van Lanen, H. A. J., Wanders, N., Tallaksen, L. M., and Van Loon, A. F.: Hydrological drought across the world: Impact of
668 climate and physical catchment structure, *Hydrol. Earth Syst. Sci.*, 17, 1715–1732, [https://doi.org/10.5194/hess-17-1715-](https://doi.org/10.5194/hess-17-1715-2013)
669 2013, 2013.

Con formato: Izquierda

Con formato: Color de fuente: Automático

Con formato: Borde: Superior: (Sin borde), Inferior: (Sin borde), Izquierda: (Sin borde), Derecha: (Sin borde), Entre : (Sin borde), Punto de tabulación: No en 3,13" 6,27"

- 670 Van Loon, A. F.: Hydrological drought explained, *Wiley Interdiscip. Rev. Water*, 2, 359–392,
671 <https://doi.org/10.1002/WAT2.1085>, 2015.
- 672 Van Loon, A. F. and Laaha, G.: Hydrological drought severity explained by climate and catchment characteristics, *J. Hydrol.*,
673 526, 3–14, <https://doi.org/10.1016/j.jhydrol.2014.10.059>, 2015.
- 674 Van Loon, A. F., Stahl, K., Di Baldassarre, G., Clark, J., Rangelroft, S., Wanders, N., Gleeson, T., Van Dijk, A. I. J. M.,
675 Tallaksen, L. M., Hannaford, J., Uijlenhoet, R., Teuling, A. J., Hannah, D. M., Sheffield, J., Svoboda, M., Verbeiren, B.,
676 Wagener, T., and Van Lanen, H. A. J.: Drought in a human-modified world: Reframing drought definitions, understanding,
677 and analysis approaches, *Hydrol. Earth Syst. Sci.*, 20, 3631–3650, <https://doi.org/10.5194/hess-20-3631-2016>, 2016.
- 678 Van Loon, A. F., Rangelroft, S., Coxon, G., Naranjo, J. A. B., Van Ogtrop, F., and Van Lanen, H. A. J.: Using paired catchments
679 to quantify the human influence on hydrological droughts, *Hydrol. Earth Syst. Sci.*, 23, 1725–1739,
680 <https://doi.org/10.5194/hess-23-1725-2019>, 2019.
- 681 Van Loon, A. F., Rangelroft, S., Coxon, G., Werner, M., Wanders, N., Di Baldassarre, G., Tjiedeman, E., Bosman, M., Gleeson,
682 T., Nauditt, A., Aghakouchak, A., Breña-Naranjo, J. A., Cenobio-Cruz, O., Costa, A. C., Fendekova, M., Jewitt, G., Kingston,
683 D. G., Loft, J., Mager, S. M., Mallakpour, I., Masih, I., Maureira-Cortés, H., Toth, E., Van Oel, P., Van Ogtrop, F., Verbist,
684 K., Vidal, J. P., Wen, L., Yu, M., Yuan, X., Zhang, M., and Van Lanen, H. A. J.: Streamflow droughts aggravated by human
685 activities despite management, *Environ. Res. Lett.*, 17, 044059, <https://doi.org/10.1088/1748-9326/ac5def>, 2022.
- 686 Wanders, N. and Wada, Y.: Human and climate impacts on the 21st century hydrological drought, *J. Hydrol.*, 526, 208–220,
687 <https://doi.org/10.1016/j.jhydrol.2014.10.047>, 2015.
- 688 Ward, P. J., de Ruiter, M. C., Mård, J., Schröter, K., Van Loon, A., Veldkamp, T., von Uexkull, N., Wanders, N., AghaKouchak,
689 A., Arnbjerg-Nielsen, K., Capewell, L., Carmen Llasat, M., Day, R., Dewals, B., Di Baldassarre, G., Huning, L. S., Kreibich,
690 H., Mazzoleni, M., Savelli, E., Teutschbein, C., van den Berg, H., van der Heijden, A., Vincken, J. M. R., Waterloo, M. J.,
691 and Wens, M.: The need to integrate flood and drought disaster risk reduction strategies, *Water Secur.*, 11,
692 <https://doi.org/10.1016/j.wasec.2020.100070>, 2020.
- 693 Zhao, G., Tian, P., Mu, X., Jiao, J., Wang, F., and Gao, P.: Quantifying the impact of climate variability and human activities on
694 streamflow in the middle reaches of the Yellow River basin, China, *J. Hydrol.*, 519, 387–398,
695 <https://doi.org/10.1016/j.jhydrol.2014.07.014>, 2014.
- 696 Zhao, Y., Feng, D., Yu, L., Wang, X., Chen, Y., Bai, Y., Hernández, H. J., Galleguillos, M., Estades, C., Biging, G. S., Radke,
697 J. D., and Gong, P.: Detailed dynamic land cover mapping of Chile: Accuracy improvement by integrating multi-temporal
698 data, *Remote Sens. Environ.*, 183, 170–185, <https://doi.org/10.1016/j.rse.2016.05.016>, 2016.

Con formato: Izquierda

Con formato: Color de fuente: Automático

Con formato: Borde: Superior: (Sin borde), Inferior: (Sin borde), Izquierda: (Sin borde), Derecha: (Sin borde), Entre : (Sin borde), Punto de tabulación: No en 3,13" 6,27"

699 **Appendix A.**

700 This appendix presents the outcomes of a comprehensive evaluation of various regression models, considering the seasonal
701 runoff as a dependent variable. The objective was to identify the key climate factors influencing the streamflow response in
702 the studied basins. Variables such as precipitation in different seasons, evapotranspiration, temperature, and the interaction
703 between temperature and precipitation were used. Additionally, a model incorporating a Box-Cox transformation of the
704 dependent variable (runoff) was examined to achieve a normal distribution in the variable.

705 After rigorous testing, it is noteworthy that the majority of the models demonstrated a singular dependency on precipitation
706 (P). We chose the model with a higher r^2 , and all variables were statistically significant at a p-value of 0.05 In Summer (Table
707 A1) this condition is achieved with model 1 (eq 2 of sect 2.3.2), where the summer runoff is modelled based on the winter
708 precipitations. In winter (table A2) the condition is achieved in model 2 (eq 3 of sect 2.3.2) where the runoff depends on the
709 winter precipitation of the present year (t) and the annual precipitation of the previous year (t-1).

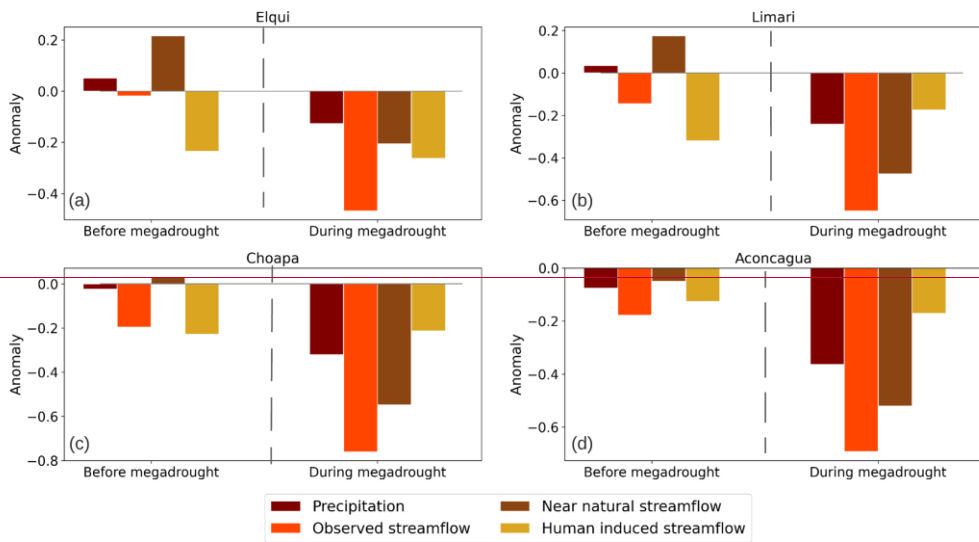
Con formato: Fuente: 9 pto

Con formato: Normal

Con formato: Izquierda

Con formato: Color de fuente: Automático

Con formato: Borde: Superior: (Sin borde), Inferior: (Sin borde), Izquierda: (Sin borde), Derecha: (Sin borde), Entre : (Sin borde), Punto de tabulación: No en 3,13" 6,27"



710

Con formato: Izquierda

Con formato: Color de fuente: Automático

Con formato: Borde: Superior: (Sin borde), Inferior: (Sin borde), Izquierda: (Sin borde), Derecha: (Sin borde), Entre : (Sin borde), Punto de tabulación: No en 3,13" 6,27"

Dependent variable: Summer runoff																				
Variables/ Models	Model 1				Model 2 (runoff Box-Cox)				Model 3				Model 4				Model 5			
	Elqui	Lim	Choap	Acon	Elqui	Lim	Choap	Acon	Elqui	Lim	Choap	Acon	Elqui	Lim	Choap	Acon	Elqui	Lim	Choap	Acon
const	-89.80*** (-5.49)	-70.05*** (-12.5)	-56.80*** (-11.34)	-61.87** (-28.38)	152*** (-0.17)	0.12 (-0.4)	138*** (-0.36)	3.57*** (-0.33)	-8.89 (-10.10)	-55.36** (-8.7)	59.92*** (-39.06)	-111.17*** (-22.99)	8.59 (-57.02)	-3.46 (-59.14)	-3.8 (-110.76)	39.82 (-90.8)	86.77 (-211.48)	174.87 (-86.45)	-158.72 (-277.96)	-218.17
P_winter(t)	0.31*** (-0.03)	0.45*** (-0.04)	0.39*** (-0.03)	0.49*** (-0.05)	0.01*** 0	0.01*** 0	0.01*** 0	0.01*** 0	0.31*** (-0.03)	0.46*** (-0.04)	0.39*** (-0.03)	0.47*** (-0.05)	0.33*** (-0.03)	0.46*** (-0.04)	0.40*** (-0.03)	0.49*** (-0.05)	0.31*** (-0.03)	0.47*** (-0.04)	0.39*** (-0.03)	0.47*** (-0.05)
P_summer(t)																				
ET_summer																				
T_mean_summer																				
TxP																				
Observations	27	27	22	26	27	27	22	26	27	27	22	26	27	27	22	26	27	27	22	26
R2	0.81	0.84	0.89	0.81	0.82	0.74	0.74	0.61	0.82	0.84	0.89	0.83	0.82	0.85	0.89	0.81	0.83	0.85	0.89	0.83
Adjusted R2	0.8	0.83	0.88	0.8	0.81	0.73	0.73	0.59	0.8	0.83	0.88	0.81	0.8	0.84	0.88	0.8	0.81	0.83	0.87	0.81
Residual Std. Error	14.2	3174	25.29	62.87	0.45	101	0.8	0.74	14.02	318	25.91	60.29	14.03	3147	25.38	63	13.92	3158	26.4	61.35
F Statistic	113.34**	130.43**	156.66***	99.65***	110.49***	69.99***	57.83***	36.78***	53.80***	65.42***	74.62***	55.72***	53.75***	67.06***	78.19***	50.07***	37.05***	23.73***	8.66***	13.94***
Note:	*p<0.1; **p<0.05; ***p<0.01; std_dv in ()																			

Table A1: results of multiple regression equations tested for representing near-natural streamflow during the reference period in the summer season

Con formato: Izquierda

Con formato: Color de fuente: Automático

Con formato: Borde: Superior: (Sin borde), Inferior: (Sin borde), Izquierda: (Sin borde), Derecha: (Sin borde), Entre : (Sin borde), Punto de tabulación: No en 3,13" 6,27"

Dependent variable: Winter runoff																				
Variables/ Models	Model 1				Model 2				Model 3 runoff (Box-Cox)				Model 4				Model 5			
	Elqui	Lim	Choap	Acon	Elqui	Lim	Choap	Acon	Elqui	Lim	Choap	Acon	Elqui	Lim	Choap	Acon	Elqui	Lim	Choap	Acon
const	1190*** (-3.67)	-15.45** (-6.23)	-10.53** (-4.02)	-11.17 (-4.14)	-5.22 (-3.49)	-30.94*** (-6.85)	-20.01*** (-4.57)	-31.44 (-20.08)	141*** (-0.42)	0.75 (-0.44)	1.13** (-0.52)	0.16 (-1.31)	-9.53** (-4.31)	-35.18*** (-12.07)	-7.67 (-7.95)	-16.03 (-53.56)	-32.84 (-20.13)	-117.70* (-58.61)	-45.62 (-40.73)	-116.79 (-82.56)
P_winter(t)	0.04* (-0.02)	0.19*** (-0.01)	0.16*** (-0.02)	0.14*** (-0.01)	0.02 (-0.01)	0.17*** (-0.02)	0.16*** (-0.01)	0.14*** (-0.02)	0.01*** 0	0.01*** 0	0.01*** 0	0.01*** 0	-0.01 (-0.02)	0.17*** (-0.02)	0.17*** (-0.01)	0.14*** (-0.03)	0.16 (-0.11)	0.57*** (-0.17)	0.23* (-0.11)	0.27** (-0.13)
P_winter(t-1)					0.09*** (-0.01)	0.06*** (-0.02)	0.03*** (-0.01)	0.03 (-0.02)	0.01*** 0	0.01*** 0	0.00*** 0	0.00*** 0	0.07*** (-0.02)	0.05* (-0.03)	0.05*** (-0.01)	0.04 (-0.03)	0.08*** (-0.02)	0.05*** (-0.02)	0.03** (-0.01)	0.03 (-0.03)
ET_winter													0.08 (-0.05)	0.05 (-0.12)	-0.15* (-0.08)	-0.12 (-0.37)				
T_mean_winter																	6.6 (-4.71)	15.65 (-9.79)	4.59 (-7.1)	32.78 (-30.42)
TxP																	-0.03 (-0.03)	-0.07** (-0.03)	-0.01 (-0.02)	-0.05 (-0.05)
Observations	26	26	25	25	26	26	25	25	26	26	25	25	26	26	25	25	26	26	25	25
R2	0.12	0.8	0.89	0.57	0.69	0.87	0.93	0.61	0.65	0.86	0.81	0.57	0.72	0.87	0.94	0.61	0.71	0.9	0.93	0.63
Adjusted R2	0.09	0.79	0.89	0.56	0.66	0.86	0.92	0.57	0.62	0.85	0.8	0.53	0.68	0.85	0.93	0.56	0.66	0.88	0.91	0.56
Residual Std. Error	9.48	15.13	9.78	32.22	5.8	12.55	8.32	3157	0.7	0.81	0.94	2.06	5.61	12.78	7.89	32.24	5.81	1151	8.62	32.18
F Statistic	3.36*	96.18***	195.83***	3106***	25.04***	75.83***	140.27***	17.14***	2100***	69.40***	47.84***	14.79***	18.72***	48.82***	104.98***	11.99***	12.99***	46.61***	65.47***	8.54***
Note:	*p<0.1; **p<0.05; ***p<0.01; std_dv in ()																			

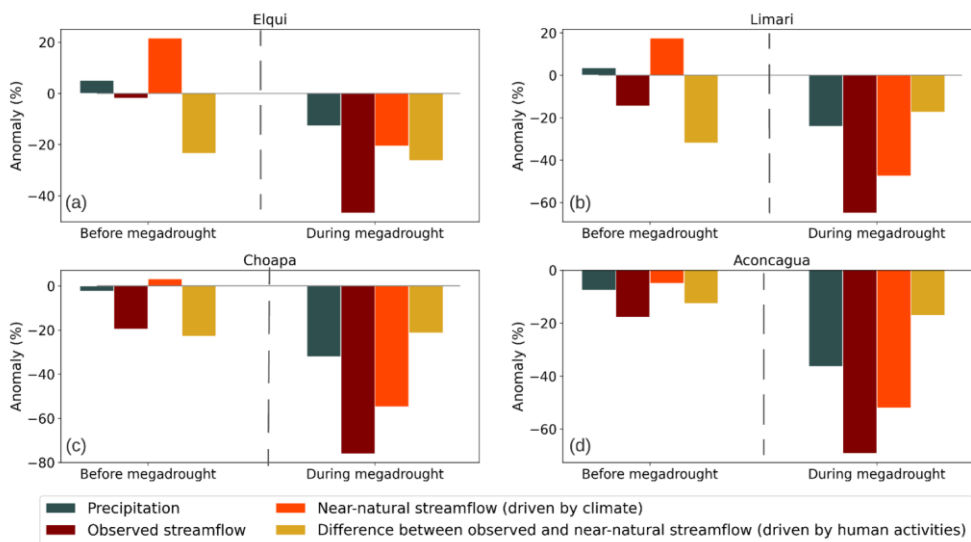
Table A2: results of multiple regression equations tested for representing near-natural streamflow during the reference period in the Winter season

Con formato: Izquierda

Con formato: Color de fuente: Automático

Con formato: Borde: Superior: (Sin borde), Inferior: (Sin borde), Izquierda: (Sin borde), Derecha: (Sin borde), Entre : (Sin borde), Punto de tabulación: No en 3,13" 6,27"

717 **Appendix B**



718
719 **Figure A1B1:** Anomalies in annual precipitation, observed streamflow, simulated near-natural streamflow and human-induced
720 streamflow change. The anomalies are presented for the evaluation period before and after the megadrought onset (1988-2009 and
721 2010-2020, respectively). For each flux, the anomalies are computed as the percentage difference with respect to their mean values
722 during the low-influence reference period (1960-1988). The graphs show these results for Elqui (a), Limari (b), Choapa (c), and
723 Aconcagua (d) Basins, **respectively**.

724 **respective**

726 **Appendix C.**

Basin	Hydrological	frequency	duration (seasons)	deficit (mm)
-------	--------------	-----------	--------------------	--------------

Con formato: Arriba: 0,39", Abajo: 0,93", Inicio de sección: Continua, Distancia del pie de página desde borde: 0,51"

Con formato: Izquierda

Con formato: Color de fuente: Automático

Con formato: Borde: Superior: (Sin borde), Inferior: (Sin borde), Izquierda: (Sin borde), Derecha: (Sin borde), Entre : (Sin borde), Punto de tabulación: No en 3,13" 6,27"

	Drought		total season	max duration	average duration	total deficit	max deficit	average deficit
Elqui	Near- natural	4.00	6.00	2.00	1.50	18.43	10.13	4.61
	Observed	4.00	14.00	10.00	3.50	63.15	53.09	15.79
	diff %	0.00%	57.14%	80.00%	57.14%	70.82%	80.92%	70.82%
Limari	Near- natural	2.00	10.00	6.00	5.00	98.39	51.69	49.20
	Observed	3.00	13.00	8.00	4.33	94.94	65.87	31.65
	diff %	33.33%	23.08%	25.00%	-15.38%	-3.64%	21.53%	-55.46%
Choapa	Near- natural	2.00	10.00	6.00	5.00	107.89	58.31	53.94
	Observed	4.00	14.00	8.00	3.50	212.76	123.74	53.19
	diff %	50.00%	28.57%	25.00%	-42.86%	49.29%	52.88%	-1.42%
Aconcagua	Near- natural	3.00	10.00	4.00	3.33	237.65	133.27	79.22
	Observed	4.00	13.00	8.00	3.25	565.61	315.06	141.40
	diff %	25.00%	23.08%	50.00%	-2.56%	57.98%	57.70%	43.98%

Table C1: drought characteristics for each basin considering the observed and simulated near natural streamflow during the megadrought period (2010-2020). The third row for each basin represents the human influence on drought characteristics as the percentage difference between the observed and the naturalized scenario

Basin	Hydrological Drought	frequency	duration (seasons)			deficit (mm)		
			total season	max duration	average duration	total deficit	max deficit	average deficit
Elqui	Near- natural	7.00	10.00	4.00	1.43	44.99	20.55	6.43
	Observed	6.00	10.00	4.00	1.67	30.46	12.73	5.08
	diff %	-16.67%	0.00%	0.00%	14.29%	-47.69%	-61.49%	-26.59%
Limari	Near- natural	4.00	7.00	4.00	1.75	68.65	50.78	17.16
	Observed	8.00	15.00	6.00	1.88	91.61	54.26	11.45
	diff %	50.00%	53.33%	33.33%	6.67%	25.06%	6.41%	-49.87%
Choapa	Near- natural	6.00	10.00	4.00	1.67	90.04	34.36	15.01
	Observed	9.00	17.00	6.00	1.89	135.96	67.42	15.11
	diff %	33.33%	41.18%	33.33%	11.76%	33.78%	49.04%	0.66%
Aconcagua	Near- natural	5.00	9.00	2.00	1.80	180.33	67.70	36.07
	Observed	9.00	13.00	3.00	1.44	468.17	110.86	52.02
	diff %	44.44%	30.77%	33.33%	-24.62%	61.48%	38.93%	30.67%

Con formato: Izquierda

Con formato: Color de fuente: Automático

Con formato: Borde: Superior: (Sin borde), Inferior: (Sin borde), Izquierda: (Sin borde), Derecha: (Sin borde), Entre : (Sin borde), Punto de tabulación: No en 3,13" 6,27"

730
731
732
733

Table C2: drought characteristics for each basin considering the observed and simulated near natural streamflow before the mega drought period (1988-2010). The third row for each basin represents the human influence on drought characteristics as the percentage difference between the observed and the naturalized scenario

Con formato: Fuente: 9 pto, Negrita
Con formato: Izquierda

Con formato: Izquierda
Con formato: Color de fuente: Automático
Con formato: Borde: Superior: (Sin borde), Inferior: (Sin borde), Izquierda: (Sin borde), Derecha: (Sin borde), Entre : (Sin borde), Punto de tabulación: No en 3,13" 6,27"